Cytosolic activation of cell death and stem rust resistance by cereal MLA-family CC-NLR proteins

Article *in* Proceedings of the National Academy of Sciences · August 2016

DOI: 10.1073/pnas.1605483113

Cytosolic activation of cell death and stem rust resistance by cereal MLA-family CC–NLR proteins

Stella Cesari[a], John Moore[a], Chunhong Chen[a], Daryl Webb[b], Sambasivam Periyannan[a], Rohit Mago[a], Maud Bernoux[a], Evans S. Lagudah[a], and Peter N. Dodds[a,1]

[a]Commonwealth Scientific and Industrial Research Organization Agriculture, Canberra, ACT 2601, Australia; and [b]Centre for Advanced Microscopy, Australian National University, Canberra, ACT 0200, Australia

Edited by Detlef Weigel, Max Planck Institute for Developmental Biology, Tubingen, Germany, and approved July 12, 2016 (received for review April 5, 2016)

Plants possess intracellular immune receptors designated "nucleotide-binding domain and leucine-rich repeat" (NLR) proteins that translate pathogen-specific recognition into disease-resistance signaling. The wheat immune receptors Sr33 and Sr50 belong to the class of coiled-coil (CC) NLRs. They confer resistance against a broad spectrum of field isolates of *Puccinia graminis* f. sp. *tritici*, including the Ug99 lineage, and are homologs of the barley powdery mildew-resistance protein MLA10. Here, we show that, similarly to MLA10, the Sr33 and Sr50 CC domains are sufficient to induce cell death in *Nicotiana benthamiana*. Autoactive CC domains and full-length Sr33 and Sr50 proteins self-associate *in planta*. In contrast, truncated CC domains equivalent in size to an MLA10 fragment for which a crystal structure was previously determined fail to induce cell death and do not self-associate. Mutations in the truncated region also abolish self-association and cell-death signaling. Analysis of Sr33 and Sr50 CC domains fused to YFP and either nuclear localization or nuclear export signals in *N. benthamiana* showed that cell-death induction occurs in the cytosol. In stable transgenic wheat plants, full-length Sr33 proteins targeted to the cytosol provided rust resistance, whereas nuclear-targeted Sr33 was not functional. These data are consistent with CC-mediated induction of both cell-death signaling and stem rust resistance in the cytosolic compartment, whereas previous research had suggested that MLA10-mediated cell-death and disease resistance signaling occur independently, in the cytosol and nucleus, respectively.

wheat stem rust | cell death | plant immunity | resistance protein | signaling

Plants have evolved effective innate immune systems to defend themselves against fast-evolving pathogens (1, 2). Plant immunity relies in part on the recognition of specific pathogen molecules, termed "effectors," that are involved in infection processes (3). Effectors are usually recognized by intracellular immune receptors called "resistance proteins"; this recognition leads to a strong immune response that often is associated with a localized programmed cell death called the "hypersensitive response" (HR).

Most known resistance proteins contain central nucleotide-binding (NB) and C-terminal leucine-rich repeat (LRR) domains (4) and are known as "NLRs." There are two major subclasses of plant NLRs: one containing N-terminal regions that resemble the intracellular domains of the *Drosophila* protein Toll and the mammalian interleukin-1 receptor protein (TIR domain), and one containing N-terminal coiled-coil (CC) domains. These N-terminal regions have been shown to be signaling domains in several plant NLRs (5–9).

Stem rust is a devastating disease caused by *Puccinia graminis* f. sp. *tritici* (*Pgt*) that threatens wheat production worldwide. Recently, two stem rust-resistance genes, *Sr33* and *Sr50*, that confer resistance to a broad spectrum of *Pgt* isolates were identified as orthologs of the barley powdery mildew resistance gene *MLA* (10, 11). More than 30 distinct *MLA* alleles have been isolated from different barley cultivars (12) and have been studied intensively. An N-terminal 160-amino acid fragment of MLA10 containing the CC domain ($CC_{1–160}$) was sufficient to trigger cell death in transient expression assays (8). A larger CC–$NB_{1–225}$ fragment was found to self-associate in yeast two-hybrid assays; a smaller $CC_{5–120}$ fragment was reported to form a stable homodimer in solution, and its crystal structure revealed a rod-shaped dimer (8), suggesting that CC self-association may be important for MLA10 signaling. Cell-death signaling by the full-length MLA10 protein or its CC–$NB_{1–225}$ domain required the cytosolic location of the protein, but in, contrast, resistance to powdery mildew disease in a transient single-cell expression assay required the presence of the protein in the nucleus (13). This finding was proposed to indicate a bifurcation between cell-death signaling and resistance signaling immediately downstream of MLA10 activation.

A wheat ortholog of the *MLA* gene family, *TmMla1*, confers resistance to wheat powdery mildew (14). Likewise, *Sr33* and *Sr50* occur at the orthologous locus in diploid wheat (*Aegilops tauschii*) and rye (*Secale cereale*), respectively, and are the first members of the MLA family known to recognize a pathogen other than powdery mildew (10, 11). MLA10, Sr33, and Sr50 proteins share ~80% amino acid sequence identity. To understand better the similarities and differences in the way these resistance proteins operate, we undertook a functional analysis of Sr33 and Sr50 with a focus on their ability to self-interact and induce cell death or disease resistance in a cell compartment-dependent manner. This analysis revealed some significant similarities with MLA in terms of CC domain signaling and *in planta* self-association but also demonstrated important differences, with Sr33 requiring cytosolic localization to confer rust resistance.

Significance

Stem rust caused by the fungus *Puccinia graminis* f. sp. *tritici* (*Pgt*) remains the major disease threat to wheat production. The Sr33 and Sr50 resistance proteins protect wheat against a broad spectrum of field isolates of *Pgt* and are closely related to the barley powdery mildew-resistance protein MLA10. Like MLA10, Sr33 and Sr50 possess signaling N-terminal domains that self-associate *in planta* and initiate cell-death signaling from the cytosol. However, Sr33 induces disease-resistance signaling from the cytosol but not from the nucleus of wheat cells, suggesting cytosolic activation of both cell death and stem rust resistance.

Author contributions: S.C., J.M., E.S.L., and P.N.D. designed research; S.C., J.M., C.C., D.W., S.P., R.M., and M.B. performed research; D.W. contributed new reagents/analytic tools; S.C., C.C., S.P., and P.N.D. analyzed data; and S.C. and P.N.D. wrote the paper.

The authors declare no conflict of interest.

This article is a PNAS Direct Submission.

[1]To whom correspondence should be addressed. Email: peter.dodds@csiro.au.

This article contains supporting information online at www.pnas.org/lookup/suppl/doi:10.1073/pnas.1605483113/-/DCSupplemental.

Results

The CC Domain of MLA10, Sr33, and Sr50 Is Sufficient for Cell-Death Induction. To investigate whether Sr33 and Sr50 function similarly to MLA in cell-death induction, we tested three N-terminal fragments of Sr33, Sr50, and MLA10, corresponding to the MLA10 1–120, 1–160, and 1–225 fragments (Fig. S1*A*). Using CC prediction software (15), we identified two coiled domains spanning roughly residues 20–50 and 115–144 in MLA10, Sr33, and Sr50 (Fig. S1*B*), suggesting that the 1–160 fragments should contain a full CC domain, whereas the 1–120 fragments may have a truncated CC domain. These N-terminal fragments were transiently expressed in *Nicotiana benthamiana* under the control of the *35S* promoter and were fused to either a C-terminal HA or CFP tag. The full CC-containing constructs of Sr33 and Sr50 (amino acids 1–160 and 1–163, respectively) triggered a strong cell-death response that was visible 40 h after agro-infiltration when fused to either CFP or HA (Fig. 1*A*). Consistent with previous reports, $MLA10_{1–160}$:HA and $MLA10_{1–160}$:CFP also induced a strong cell-death response. A positive control protein, the rice autoactive CC–NLR RGA4, produced a strong cell-death response, but its inactive $T_{500}M/Y_{501}H/G_{502}D$ mutant ($rga4_{TYG/MHD}$) did not (16, 17). Expression of the CC–NB fragments of Sr33 (residues 1–225), Sr50 (1–228), and MLA10 (1–225) also triggered a cell-death response (Fig. 1*B*), but the truncated CC domains of MLA10 (1–120), Sr33 (1–120), and Sr50 (1–123) fused to HA or CFP did not induce cell death (Fig. 1*C* and Fig. S2*A*). Western blot analysis indicated that all fusion proteins were properly expressed (Fig. 2 and Fig. S3 *A–C*). Full-length *Sr33* and *Sr50* cDNA constructs also induced cell death when driven by the 35S promoter (Fig. 1*C* and Figs. S2*B* and S3*D*), whereas expression of the genomic constructs under their native cereal promoters led to very low or undetectable protein expression and no cell-death response in *N. benthamiana* (Figs. S2*B* and S3*D*).

The Sr33, Sr50, and MLA10 CC Domains Self-Associate *in Planta*. Although the truncated $CC_{5–120}$ fragment of MLA10 was reported to homodimerize in solution, and its CC-$NB_{1–225}$ domain was reported to self-interact in a yeast two-hybrid assay (8), self-interaction has not been demonstrated with the minimal active $CC_{1–160}$ domain. In contrast to MLA10, self-interaction of the Sr33 CC-$NB_{1–225}$ domain, the $CC_{1–120}$ domain, and the $CC_{1–160}$ domain was not detected by yeast two-hybrid assay (10). We tested the active CC and CC-NB fragments of MLA10 and Sr50 in a GAL4-based yeast two-hybrid system but did not observe evidence of self-interaction, although all fusion proteins were expressed (Fig. S4). Self-interaction was detected for the rice Resistance Gene Analog 5 (RGA5) $CC_{1–228}$ and L6-TIR domain, the positive controls in this experiment (Fig. S4) (7, 17).

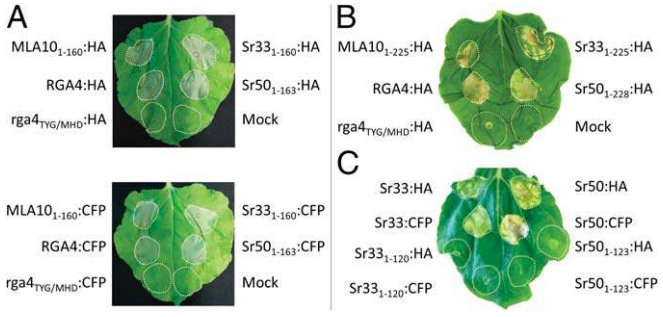

Fig. 1. The full CC domains of MLA10, Sr33, and Sr50 are sufficient for autoactivity *in planta*. Indicated fragments of the MLA10, Sr33, and Sr50 proteins fused to HA or CFP were transiently expressed in *N. benthamiana* leaves by *Agrobacterium tumefaciens* infiltration along with the autoactive RGA4:HA or RGA4:CFP positive controls and the inactive $rga4_{TYG/MHD}$:HA or $rga4_{TYG/MHD}$:CFP or mock inoculation as negative controls. Pictures were taken 3 d (*A*) or 5 d (*B* and *C*) after infiltration. Equivalent results were obtained in three independent experiments.

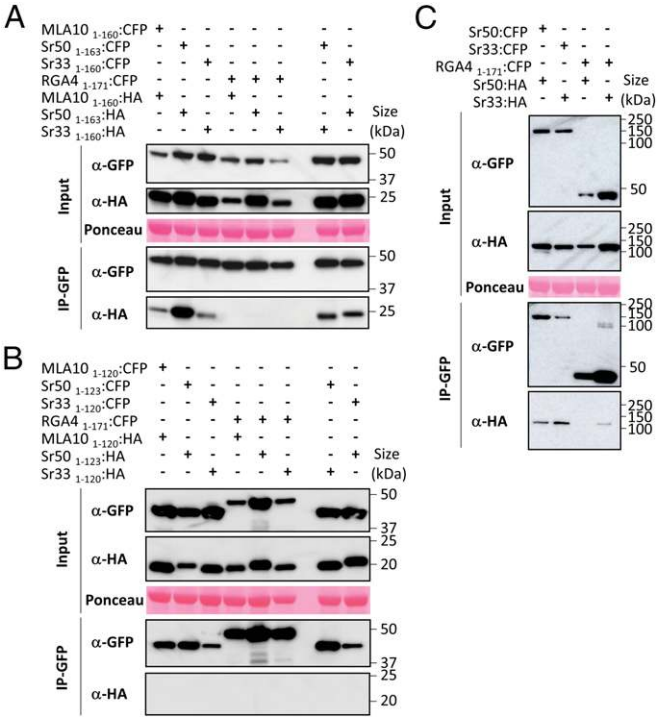

Fig. 2. The full CC domains of Sr33, Sr50, and MLA10 can self-associate *in planta*. (*A*) The full CC domains of MLA10, Sr33, and Sr50 fused to CFP or HA tags were transiently expressed in *N. benthamiana* leaves in the indicated combinations (+, agro-infiltrated construct; –, non–agro-infiltrated construct), and proteins were extracted after 24 h. Tagged proteins were detected in the extract (input) and after immunoprecipitation with anti-GFP beads (IP-GFP) by immunoblotting with anti-HA (α-HA) and anti-GFP (α-GFP) antibodies. The RGA4 CC fused to CFP was used as a control for specificity. Protein loading in the input is shown by Ponceau staining of the large RuBisCO (ribulose-1,5-bisphosphate carboxylase/oxygenase) subunit. The experiment was carried out three times with identical results. (*B*) The truncated CC domains of MLA10, Sr33, and Sr50 fused to CFP or HA were transiently expressed in *N. benthamiana* leaves in the indicated combinations. Samples were processed as described in *A*. The experiment was carried out twice with identical results. (*C*) The procedure described in *A* was applied to the full-length Sr33 and Sr50 proteins.

To determine whether these CC domains could self-associate *in planta*, we performed coimmunoprecipitation experiments in *N. benthamiana* using the auto-active CC domains of Sr33, Sr50, and MLA10 fused to CFP or HA tags. Proper expression of all proteins was verified by immunoblotting using anti-GFP and anti-HA antibodies (Fig. 2*A*). CFP-fused proteins were enriched after immunoprecipitation with anti-GFP beads, and $MLA10_{1–160}$:HA, $Sr33_{1–160}$:HA, and $Sr50_{1–163}$:HA specifically coprecipitated with $MLA10_{1–160}$:CFP, $Sr33_{1–160}$:CFP, and $Sr50_{1–163}$:CFP, respectively, but not with $RGA4_{1–171}$:CFP (17), which was used as a negative control for binding specificity (Fig. 2*A*). These results show that the CC domains of MLA10, Sr33, and Sr50 form specific homocomplexes *in planta*. Interestingly, Sr33 and Sr50 CC domains also formed heterocomplexes when coexpressed *in planta* (Fig. 2*A*). This coexpression did not impair cell-death induction (Fig. S5*A*).

We also tested whether the truncated CC domains, which are inactive in cell-death signaling, would retain self-association or hetero-association in *N. benthamiana*. Although all fusion proteins were detected in leaf extracts by immunoblotting with anti-GFP or anti-HA antibodies, and CFP-tagged proteins were precipitated by anti-GFP beads, the HA-tagged proteins did not coprecipitate with any of the CFP-tagged proteins (Fig. 2*B* and Fig. S5*B*). Thus,

self-association *in planta* appears to be a property limited to the active signaling fragments of these proteins.

Full-Length Sr33 and Sr50 Proteins also Self-Associate *in Planta*. The full-length MLA1 protein was also shown to self-associate *in planta* (8), so we tested full-length Sr33 and Sr50 self-association by coimmunoprecipitation (Fig. 2*C*). Immunoblotting using anti-GFP and anti-HA antibodies showed expression of all proteins in the input, and immunoprecipitation with anti-GFP beads resulted in the pulldown of CFP-fused proteins and coprecipitation of the HA-tagged protein. Although Sr33:HA showed a low level of unspecific binding to $RGA4_{1–171}$:CFP and to the anti-GFP beads (Fig. 2*C* and Fig. S5*C*), an enrichment of coimmunoprecipitated Sr33:HA protein was observed in the presence of Sr33:CFP (Fig. 2*C* and Fig. S5*C*). These results suggest that the Sr33 and Sr50 proteins also form homocomplexes *in planta*. Full-length Sr33 and Sr50 proteins also could form heterocomplexes in *N. benthamiana* (Fig. S5*D*), but this interaction did not inhibit cell-death induction (Fig. S5*A*).

Residues Within the 120–144 Region of Sr33 CC Domain Are Crucial for Self-Association and Autoactivity. The data presented above suggest that the region corresponding to MLA10 residues 120–160 is important for cell-death signaling activity and self-association. To test this suggestion further, we generated six different mutations within this region of Sr33 (Fig. 3*A*). In five mutants we exchanged conserved hydrophobic residues for negatively charged glutamate residues, and in one mutant we exchanged a conserved six amino acid hydrophilic stretch (RRDRNK) for alanine residues. These mutations were independently introduced in both the $CC_{1–160}$ domain and the full-length Sr33 protein, and transient expression experiments in *N. benthamiana* showed that all mutations impaired cell-death induction by both CC and full-length proteins (Fig. 3*B*), although all proteins were well expressed (Fig. 3*C* and Fig. S3*E*). In addition, coimmunoprecipitation assays revealed that all the mutations disrupted or strongly inhibited Sr33 CC self-association *in planta* (Fig. 3*C*). Taken together, these data indicate a crucial role of this region for both signaling and self-association.

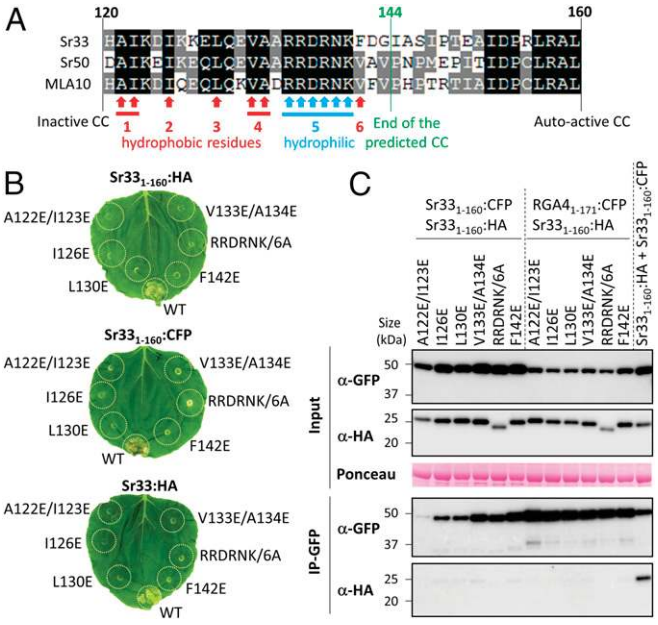

Fig. 3. Residues within the 120–144 CC region of Sr33 are crucial for self-association and autoactivity. (*A*) Alignment showing the 120–160 fragment of MLA10, Sr33, and Sr50. Six mutations (numbered 1–6) were generated in which conserved hydrophobic residues (red) were replaced by glutamate, or a hydrophilic stretch (blue) was replaced by alanines. (*B*) WT and mutated constructs of the Sr33 $CC_{1–160}$ domain or full-length protein fused to HA or CFP were transiently expressed in *N. benthamiana*, and cell death was visualized after 4 d. Equivalent results were obtained in three independent experiments. (*C*) The indicated mutants of the Sr33 $CC_{1–160}$ domain fused to CFP or HA tags were coexpressed in *N. benthamiana* and analyzed by coimmunoprecipitation as described in Fig. 2*A*. $RGA4_{1–171}$:CFP was used as a control for specificity, and WT Sr33$_{1–160}$:HA and Sr33$_{1–160}$:CFP were used as positive controls. Three independent experiments gave equivalent results.

Cytosolic Localization of MLA10, Sr33, and Sr50 CC Domains Is Required for Cell-Death Induction. The MLA10 full-length protein and its CC-$NB_{1–225}$ domain induce cell-death signaling in the cytoplasm of *N. benthamiana* cells (13). To test whether the smaller CC-containing autoactive domains also induce cell-death signaling in the cytosol, we transiently expressed $MLA10_{1–160}$:YFP, Sr33$_{1–160}$:YFP, and $Sr50_{1–163}$:YFP in *N. benthamiana* fused to a nuclear localization signal (NLS), a mutated NLS (nls) (18), a nuclear export signal (NES), or a mutated NES (nes) (19). Upon expression of the YFP:NLS-fused CC domains, specific YFP fluorescence was detected exclusively in the nuclei of *N. benthamiana* cells (Fig. 4*A* and Fig. S6*A*). In contrast, the CC domains fused to YFP:NES were effectively, although not completely, excluded from nuclei, with fluorescence detected mostly in the cytosol. CC:YFP domains fused to mutated nls and nes variants fluoresced in both the cytosol and nuclei (Fig. 4*A* and Fig. S6*A*). Cell-death assays revealed that forced nuclear localization of all CC domains reduced their cell-death activity compared with other fusions with YFP:NES, YFP:nes, or YFP:nls (Fig. 4*B*). This cell-death reduction was less pronounced for the Sr50 CC domain than for the MLA10 and Sr33 CC domains (Fig. 4*B*). However, the strongest cell-death response triggered by the Sr50 CC domain was observed when it was fused to the NES, indicating that nuclear localization of Sr50 CC domain is not required for its signaling activity. Protein expression of all constructs was verified by immunoblotting (Fig. S3*F*). The NES-fused constructs consistently showed lower protein accumulation but nevertheless gave the strongest cell-death phenotype, suggesting that cell-death and protein-degradation processes had already been activated at the time of sampling. These results indicate that the MLA10, Sr33, and Sr50 CC domains activate cell-death signaling from the cytosol.

Sr33 Induces Stem Rust Resistance in the Cytosol of Wheat Cells. Previous reports showed that full-length MLA10 locates to both the cytoplasm and the nucleus of transiently transformed barley leaf epidermal cells (20) and that, in contrast to cell-death signaling, the nuclear pool is required for its powdery mildew resistance activity (13, 20). To examine the subcellular distribution of Sr33 and to identify the compartment in which it induces disease resistance, we stably transformed wheat with constructs carrying the genomic sequence of *Sr33* driven by its native promoter (*pSr33*) and fused with either YFP venus (YFPv), YFPv:NLS, YFPv:nls, YFPv:NES, or YFPv:nes, as well as a construct containing *YFPv* under the control of the *pSr33* promoter. Progeny of six independent T0 transgenic lines for each construct were assessed for resistance to *Pgt* race 98-1,2,3,5,6 (and Fig. 5*A* and Table S1). T1 plants derived from three independent T0 lines expressing *Sr33:YFP* segregated for stem rust resistance, confirming the function of the YFPv-fused Sr33 protein. All transgenic lines carrying the *Sr33:YFPv:NES*, *Sr33:YFPv:nes*, or *Sr33:YFPv:nls* constructs gave rise to resistant T1 plants. However, all transformed lines containing the *Sr33:YFPv:NLS* construct were fully susceptible, similar to untransformed wheat or plants carrying the *YFPv* construct (Fig. 5*A* and Table S1). Immunoblot analysis revealed that all the YFP fusion constructs were expressed, with no YFPv cleavage observed (Fig. 5*B*).

Using confocal microscopy we observed that Sr33:YFPv accumulated mostly in the cytosol of leaf epidermal cells of the transgenic lines and was only weakly visible in a small proportion of nuclei (Fig. S6*B*). However, it was difficult to visualize Sr33:YFPv fluorescence in mesophyll cells, which are the main site of interaction with *Pgt* during infection (21). Therefore, we isolated

PLANT BIOLOGY

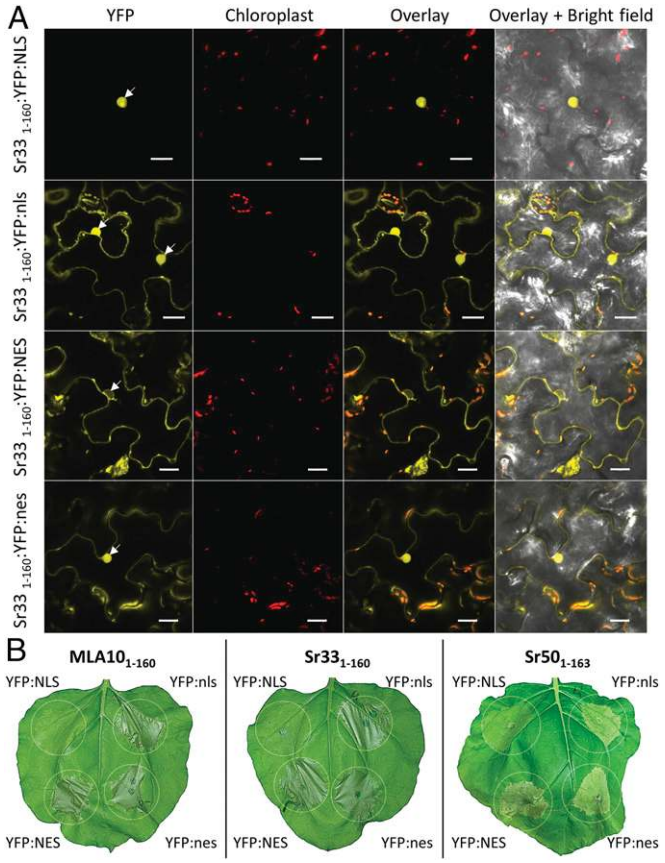

Fig. 4. The CC domains of Sr33, Sr50, and MLA10 induce cell-death signaling in the cytosol of *N. benthamiana* cells. (*A*) Fluorescence microscopy images (20 h postinfiltration) of the localization of the Sr33 $CC_{1–160}$ domain fused to YFP:NLS, YFP:nls, YFP:NES, or YFP:nes in transiently transformed *N. benthamiana* leaf epidermal cells. Fluorescence channels for YFP and chloroplasts are merged on the overlay picture, and all channels are merged on the overlay + bright-field picture. White arrows indicate nuclei. (Scale bars, 20 μm.) (*B*) MLA10 $CC_{1–160}$, Sr33 $CC_{1–160}$, and Sr50 $CC_{1–163}$ domains fused to YFP:NLS, YFP:nls, YFP:NES, or YFP:nes were transiently expressed in *N. benthamiana* leaves by *A. tumefaciens* infiltration. Pictures were taken 40 h after infiltration. Equivalent results were obtained in three independent experiments.

mesophyll protoplasts from the T1 transgenic plants. We observed exclusive localization of YFPv fluorescence in the cytosol in these cells, indicating that Sr33:YFPv proteins are largely excluded from the nucleus (Fig. 6). By contrast, YFPv expressed under the control of the *Sr33* promoter exhibited a nucleo-cytosolic localization pattern in both leaf epidermal cells and mesophyll protoplasts (Fig. 6 and Fig. S6*B*).

The Sr33:YFPv:NLS construct showed clear nuclear accumulation and undetectable cytosolic YFPv fluorescence in all epidermal or mesophyll cells, demonstrating that the NLS effectively targets Sr33 to the nucleus (Fig. 6 and Fig. 6*B*). Sr33:YFPv:nls proteins showed cytosolic and nuclear fluorescence in both epidermal and mesophyll cells, suggesting that the mutated nls retains some nuclear targeting activity (Fig. 6 and Fig. 6*B*). The subcellular fluorescence distribution of cells expressing Sr33:YFPv:NES and Sr33:YFPv:nes were indistinguishable from Sr33:YFPv, and these proteins were present exclusively in the cytosol (Fig. 6 and Fig. 6*B*). Taken together, these results show that Sr33 localizes to and induces stem rust resistance in the cytosol of wheat cells.

Discussion

In this study, we provide evidence that the CC domains of MLA10, Sr33, and Sr50 are active in cell-death signaling and self-associate *in planta*. Similarly, full-length Sr33 and Sr50 proteins trigger a pathogen-independent cell-death response in *N. benthamiana* and self-associate *in planta* in the absence of recognized avirulence effector. These results are consistent with previous reports showing that MLA10 full-length protein displays autoactivity and self-associates in coimmunoprecipitation experiments (8, 13). However, because these proteins are autoactive in *N. benthamiana*, it is not clear whether this self-association represents a pre- or postactivation event, and it remains possible that the self-association of these NLR proteins is triggered by effector recognition. These results also are in line with the idea that plant NLR protein oligomerization plays an important role in their activation or repression processes. Indeed, together with MLA, previous studies on a number of immune receptors such as N, RPS5, Prf, RB, L6, RPS4/RRS1, or RGA4/RGA5 indicate that their N-terminal domains provide a self-association platform (7, 17, 22–26). In L6, MLA10, and RPS4, a clear link between CC/TIR self-interaction and cell-death signaling was observed (7, 8, 26), whereas for the NLR hetero-pairs RPS4/RRS1 and RGA4/RGA5, hetero-interactions are crucial to regulate the activity of the signaling-competent NLR partner (17, 26).

Although the CC domains of MLA10, Sr33, and Sr50 trigger cell death and self-associate *in planta*, their truncated CC domains do not self-associate in coimmunoprecipitation assays and are inactive in cell-death signaling. Furthermore, mutations within the 120–144 region of the predicted CC domain of Sr33 inhibited both cell-death induction and self-association. Therefore these truncated CC domains appear to lack important residues for cell-death induction and self-association. It was previously reported that a similar truncated domain of the MLA10 CC (5–120) forms a dimer in solution, and a dimeric crystal structure was solved (8). However, given that this domain lacks signaling activity, and does not self-associate *in planta*, it is not clear how these structural observations relate to the biological activity of the protein. We believe that further structural investigations of an active CC domain will be necessary to unravel the molecular bases for MLA10, Sr33, and Sr50 CC self-association.

We did not detect self-association of inactive truncated CC, active CC, or CC–NB domains of Sr33 (10), Sr50, or MLA10 using a Gal4-based yeast-two-hybrid assay. Self-interaction of the MLA10 $CC–NB_{1–225}$ domain was previously reported using a LexA-based yeast two-hybrid system (8), which may be more sensitive. However, it is possible that self-association of the active domains of MLA10, Sr33, and Sr50 may require additional uncharacterized plant proteins.

We also found that the Sr33 and Sr50 CC domains or full-length proteins can hetero-associate in coimmunoprecipitation assays. Because *Sr33* and *Sr50* are derived from diploid wheat and

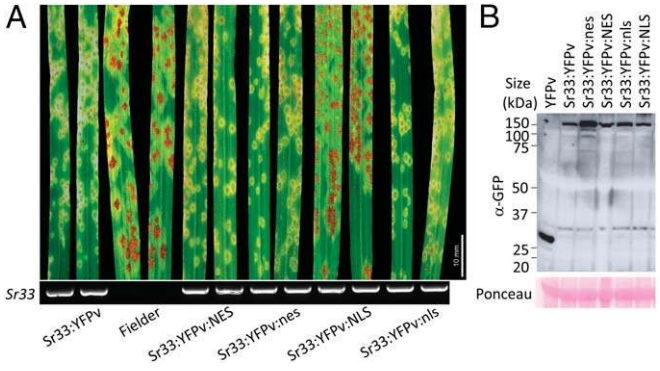

Fig. 5. Sr33 induces disease-resistance signaling from the cytosol of wheat cells. (*A*) Untransformed Fielder and two independent T1 transgenic lines per construct expressing Sr33 fused to YFPv, YFPv:NLS, YFPv:nls, YFPv:NES, or YFPv:nes plants were inoculated with *Pgt* strain 98-1,2,3,5,6 at the two-leaf stage. Pictures were taken 13 d after inoculation. The presence of the transgenes was determined by PCR with Sr33-specific primers. (*B*) Immunoblot of transgenic wheat seedlings expressing YFP-tagged proteins detected with anti-GFP.

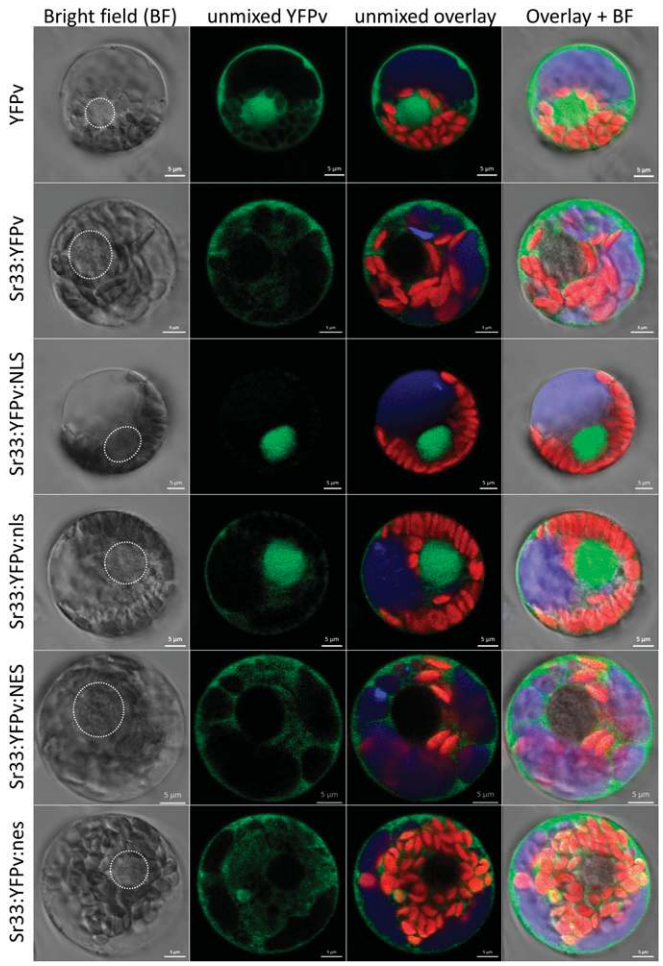

Fig. 6. Localization of Sr33 fusion proteins in wheat mesophyll protoplasts. (*A*) Linear unmixing confocal images showing the localization of Sr33 fused to the YFPv, YFPv:NLS, YFPv:nls, YFPv:NES, or YFPv:nes in transgenic wheat mesophyll protoplasts. Protoplasts were isolated from 10- to 14-d-old T1 transgenic plants and were observed within 8 h following isolation. YFP-specific fluorescence appears in green; specific vacuolar and chloroplastic autofluorescence emissions are shown in blue and red, respectively. White circles mark nuclei locations on bright-field pictures. (Scale bars, 5 μm.)

rye, respectively (10, 11), these genes do not naturally occur together in the same plant, but both have been introgressed into cultivated wheat to provide stem rust resistance. Their hetero-association *in planta* raises the possibility that they could interfere functionally, because such interference has been reported for the powdery mildew resistance gene *Pm8*, derived from rye, and its wheat ortholog *Pm3*, which also form heterocomplexes (27).

NLR proteins have been observed in a wide diversity of subcellular compartments. Many, such as N (28, 29), SNC1 (30), Pikh-1/Pikh-2 (31), Rx (32), Pb1 (33), MLA10 (20), and Rp1-D21, show a nucleo-cytoplasmic localization (34). Some, such as RGA4/RGA5, are localized mainly in the cytosol (17). In the presence of their corresponding effectors, R3a is relocalized from the cytosol to the endosome (35), whereas RRS1 is stabilized in the nucleus (36, 37). RPS4, which functions together with RRS1, distributes between endomembranes and nuclei, and its nuclear localization is required for AvrRPS4 recognition (38). Rpm1 (39), RPS2 (40), RPS5 (41), and Pit (42) are associated with the plasma membrane, whereas L6 and M are addressed to the Golgi membrane and tonoplast, respectively (43). This observation raises a fundamental question: What is the link between NLR localization and cell-death and/or disease-resistance signaling activity?

Here we found that the MLA10, Sr33, and Sr50 CC domains induce cell-death signaling in the cytosol of *N. benthamiana* cells. This finding is consistent with previous reports of cell-death induction by the full-length MLA10 protein or the MLA10 CC-NB in *N. benthamiana* (13). However, in stably transformed wheat, Sr33 confers stem rust resistance when it is located in the cytosol but not when it is confined to the nucleus. This effect is consistent with the cell-death signaling result but differs from the observations that nuclear-localized MLA10 is sufficient to confer resistance to *Blumeria graminis* in transient expression assays based on biolistic transformation of barley epidermal cells, while nuclear-excluded MLA10 cannot confer resistance (13, 20). Bai et al. (13) proposed a bifurcation of MLA10-triggered cell-death and disease-resistance signaling immediately after the receptor activation, so that MLA10 could directly trigger cell death in the cytosol and also could trigger a separate response leading to resistance in the nucleus. Another factor possibly contributing to these differing observations is that the corresponding effectors may have different localizations, with AvrMLA10 perhaps being localized to the nucleus and AvrSr33 to the cytosol and thus requiring nuclear or cytosolic receptors, respectively, for their recognition. It has been shown that exclusion of PopP2 from the nucleus impairs its recognition by RPS4 and RRS1, indicating that colocalization of the effector and NLR is required to trigger the HR in this system (44). Given that the HvWRKY1/2 and MYB6 transcription factors interact with the MLA10 CC domain (20, 45), it is possible that these nuclear proteins are guardees/decoys that are necessary for effector perception. Indeed, recent findings suggest that transcription factors such as WRKY and MYB are common integrated domains/decoys in plant NLR proteins, indicating that they could be common effector targets (46–48). Previous yeast two-hybrid assays did not detect any interaction of the Sr33 CC domain with HvWRKY1, HvWRKY2, or their wheat orthologs (10).

In terms of compartment-dependent activation, Sr33 is more similar to the potato CC–NLR Rx, a nucleo-cytoplasmic protein that recognizes the potato virus X (PVX) coat protein (CP) (32, 49). Rx interacts with the small cytosolic GTPase RanGAP2, which is required for Rx function (50, 51) and affects Rx nucleo-cytoplasmic distribution (49). Overexpression of RanGAP2 sequesters Rx in the cytosol, leading to enhanced Rx activity, whereas expression of NLS-fused RanGAP2 leads to Rx accumulation in the nucleus and inhibits Rx function (49). Likewise, fusion of an NLS to Rx significantly compromised its activity, whereas an NES fusion had a minimal effect (32). Furthermore, nuclear-targeted PVX CP does not induce the Rx-dependent HR, suggesting that both pathogen recognition and resistance signaling take place in the cytoplasm (32). However, unlike Sr33, Rx induces cell-death signaling through its NB domain, not through the CC domain (52). Therefore, although Rx and Sr33 display certain similarities, their signaling components and regulatory mechanisms may differ. Considering the wide diversity of NLR subcellular localizations and the existence of several identified signaling domains among NLRs, multiple disease-signaling pathways may exist.

Our study suggests that the AvrSr33 effector would be directly or indirectly recognized by the cytosolic pool of Sr33 and that the CC domain of the activated receptor would interact with cytosolic signaling partners to initiate both disease resistance and cell death. Subsequent downstream signaling pathway branches may be responsible for responses in different cellular compartments, such as transcriptional changes in the nucleus.

Methods

Details of the methods used are provided in *SI Methods*, including plant growth and infection assay conditions, constructs, yeast two-hybrid analysis, transient expression in *N. benthamiana*, protein extraction immunoblot and coimmunoprecipitation, wheat transformation, protoplast isolation, confocal microscopy, and accession numbers. Primers are listed in Table S2. Details of constructs are given in Table S3.

ACKNOWLEDGMENTS. We thank T. Richardson, S. Louis, D. Bhatt, X. Xia, and K. Newell for technical assistance; Drs. A. Ashton, M. Ayliffe, X. Zhang, and S. Williams for helpful comments and discussions; and Prof. P. Schulze-Lefert and Dr. S. Rivas for providing MLA10 cDNA and binary vectors, respectively. S.C. was supported by a Contrat Jeune Scientifique Postdoctoral Fellowship from L'Institut National de la Recherche Agronomique. M.B. was a recipient of Discovery Early Career Research Award DE130101292 from the Australian Research Council. This work also was supported by funding from the Durable Rust Resistance in Wheat Project and Grains Research and Development Corporation Grant CSP00161.

1. Dodds PN, Rathjen JP (2010) Plant immunity: Towards an integrated view of plant-pathogen interactions. *Nat Rev Genet* 11(8):539–548.
2. Jones JDG, Dangl JL (2006) The plant immune system. *Nature* 444(7117):323–329.
3. Kamoun S (2007) Groovy times: Filamentous pathogen effectors revealed. *Curr Opin Plant Biol* 10(4):358–365.
4. Takken FL, Goverse A (2012) How to build a pathogen detector: Structural basis of NB-LRR function. *Curr Opin Plant Biol* 15(4):375–384.
5. Swiderski MR, Birker D, Jones JDG (2009) The TIR domain of TIR-NB-LRR resistance proteins is a signaling domain involved in cell death induction. *Mol Plant Microbe Interact* 22(2):157–165.
6. Krasileva KV, Dahlbeck D, Staskawicz BJ (2010) Activation of an *Arabidopsis* resistance protein is specified by the in planta association of its leucine-rich repeat domain with the cognate oomycete effector. *Plant Cell* 22(7):2444–2458.
7. Bernoux M, et al. (2011) Structural and functional analysis of a plant resistance protein TIR domain reveals interfaces for self-association, signaling, and autoregulation. *Cell Host Microbe* 9(3):200–211.
8. Maekawa T, et al. (2011) Coiled-coil domain-dependent homodimerization of intracellular barley immune receptors defines a minimal functional module for triggering cell death. *Cell Host Microbe* 9(3):187–199.
9. Wang G-F, et al. (2015) Molecular and functional analyses of a maize autoactive NB-LRR protein identify precise structural requirements for activity. *PLoS Pathog* 11(2): e1004674.
10. Periyannan S, et al. (2013) The gene Sr33, an ortholog of barley Mla genes, encodes resistance to wheat stem rust race Ug99. *Science* 341(6147):786–788.
11. Mago R, et al. (2015) The wheat Sr50 gene reveals rich diversity at a cereal disease resistance locus. *Nat Plants* 1(12):15186.
12. Seeholzer S, et al. (2010) Diversity at the Mla powdery mildew resistance locus from cultivated barley reveals sites of positive selection. *Mol Plant Microbe Interact* 23(4):497–509.
13. Bai S, et al. (2012) Structure-function analysis of barley NLR immune receptor MLA10 reveals its cell compartment specific activity in cell death and disease resistance. *PLoS Pathog* 8(6):e1002752.
14. Jordan T, et al. (2011) The wheat Mla homologue TmMla1 exhibits an evolutionarily conserved function against powdery mildew in both wheat and barley. *Plant J* 65(4):610–621.
15. Lupas A, Van Dyke M, Stock J (1991) Predicting coiled coils from protein sequences. *Science* 252(5009):1162–1164.
16. Cesari S, et al. (2013) The rice resistance protein pair RGA4/RGA5 recognizes the *Magnaporthe oryzae* effectors AVR-Pia and AVR1-CO39 by direct binding. *Plant Cell* 25(4):1463–1481.
17. Césari S, et al. (2014) The NB-LRR proteins RGA4 and RGA5 interact functionally and physically to confer disease resistance. *EMBO J* 33(17):1941–1959.
18. Lanford RE, Butel JS (1984) Construction and characterization of an SV40 mutant defective in nuclear transport of T antigen. *Cell* 37(3):801–813.
19. Wen W, Meinkoth JL, Tsien RY, Taylor SS (1995) Identification of a signal for rapid export of proteins from the nucleus. *Cell* 82(3):463–473.
20. Shen Q-H, et al. (2007) Nuclear activity of MLA immune receptors links isolate-specific and basal disease-resistance responses. *Science* 315(5815):1098–1103.
21. Garnica DP, Nemri A, Upadhyaya NM, Rathjen JP, Dodds PN (2014) The ins and outs of rust haustoria. *PLoS Pathog* 10(9):e1004329.
22. Ade J, DeYoung BJ, Golstein C, Innes RW (2007) Indirect activation of a plant nucleotide binding site-leucine-rich repeat protein by a bacterial protease. *Proc Natl Acad Sci USA* 104(7):2531–2536.
23. Gutierrez JR, et al. (2010) Prf immune complexes of tomato are oligomeric and contain multiple Pto-like kinases that diversify effector recognition. *Plant J* 61(3):507–518.
24. Mestre P, Baulcombe DC (2006) Elicitor-mediated oligomerization of the tobacco N disease resistance protein. *Plant Cell* 18(2):491–501.
25. Chen Y, Liu Z, Halterman DA (2012) Molecular determinants of resistance activation and suppression by *Phytophthora infestans* effector IPI-O. *PLoS Pathog* 8(3):e1002595.
26. Williams SJ, et al. (2014) Structural basis for assembly and function of a heterodimeric plant immune receptor. *Science* 344(6181):299–303.
27. Hurni S, et al. (2014) The powdery mildew resistance gene *Pm8* derived from rye is suppressed by its wheat ortholog *Pm3*. *Plant J* 79(6):904–913.
28. Burch-Smith TM, et al. (2007) A novel role for the TIR domain in association with pathogen-derived elicitors. *PLoS Biol* 5(3):e68.
29. Caplan JL, Mamillapalli P, Burch-Smith TM, Czymmek K, Dinesh-Kumar SP (2008) Chloroplastic protein NRIP1 mediates innate immune receptor recognition of a viral effector. *Cell* 132(3):449–462.
30. Cheng YT, et al. (2009) Nuclear pore complex component MOS7/Nup88 is required for innate immunity and nuclear accumulation of defense regulators in Arabidopsis. *Plant Cell* 21(8):2503–2516.
31. Zhai C, et al. (2014) Function and interaction of the coupled genes responsible for Pik-h encoded rice blast resistance. *PLoS One* 9(6):e98067.
32. Slootweg E, et al. (2010) Nucleocytoplasmic distribution is required for activation of resistance by the potato NB-LRR receptor Rx1 and is balanced by its functional domains. *Plant Cell* 22(12):4195–4215.
33. Inoue H, et al. (2013) Blast resistance of CC-NB-LRR protein Pb1 is mediated by WRKY45 through protein-protein interaction. *Proc Natl Acad Sci USA* 110(23):9577–9582.
34. Wang G-F, Balint-Kurti PJ (2015) Cytoplasmic and nuclear localizations are important for the hypersensitive response conferred by maize autoactive Rp1-D21 protein. *Mol Plant Microbe Interact* 28(9):1023–1031.
35. Engelhardt S, et al. (2012) Relocalization of late blight resistance protein R3a to endosomal compartments is associated with effector recognition and required for the immune response. *Plant Cell* 24(12):5142–5158.
36. Deslandes L, et al. (2003) Physical interaction between RRS1-R, a protein conferring resistance to bacterial wilt, and PopP2, a type III effector targeted to the plant nucleus. *Proc Natl Acad Sci USA* 100(13):8024–8029.
37. Tasset C, et al. (2010) Autoacetylation of the *Ralstonia solanacearum* effector PopP2 targets a lysine residue essential for RRS1-R-mediated immunity in *Arabidopsis*. *PLoS Pathog* 6(11):e1001202.
38. Wirthmueller L, Zhang Y, Jones JDG, Parker JE (2007) Nuclear accumulation of the *Arabidopsis* immune receptor RPS4 is necessary for triggering EDS1-dependent defense. *Curr Biol* 17(23):2023–2029.
39. Gao Z, Chung E-H, Eitas TK, Dangl JL (2011) Plant intracellular innate immune receptor Resistance to *Pseudomonas syringae* pv. maculicola 1 (RPM1) is activated at, and functions on, the plasma membrane. *Proc Natl Acad Sci USA* 108(18):7619–7624.
40. Axtell MJ, Staskawicz BJ (2003) Initiation of RPS2-specified disease resistance in *Arabidopsis* is coupled to the AvrRpt2-directed elimination of RIN4. *Cell* 112(3): 369–377.
41. Qi D, DeYoung BJ, Innes RW (2012) Structure-function analysis of the coiled-coil and leucine-rich repeat domains of the RPS5 disease resistance protein. *Plant Physiol* 158(4):1819–1832.
42. Kawano Y, et al. (2014) Palmitoylation-dependent membrane localization of the rice resistance protein Pit is critical for the activation of the small GTPase OsRac1. *J Biol Chem* 289(27):19079–19088.
43. Takemoto D, et al. (2012) N-terminal motifs in some plant disease resistance proteins function in membrane attachment and contribute to disease resistance. *Mol Plant Microbe Interact* 25(3):379–392.
44. Sohn KH, et al. (2014) The nuclear immune receptor RPS4 is required for RRS1SLH1-dependent constitutive defense activation in Arabidopsis thaliana. *PLoS Genet* 10(10): e1004655.
45. Chang C, et al. (2013) Barley MLA immune receptors directly interfere with antagonistically acting transcription factors to initiate disease resistance signaling. *Plant Cell* 25(3):1158–1173.
46. Cesari S, Bernoux M, Moncuquet P, Kroj T, Dodds PN (2014) A novel conserved mechanism for plant NLR protein pairs: The "integrated decoy" hypothesis. *Front Plant Sci* 5(606):606.
47. Kroj T, Chanclud E, Michel-Romiti C, Grand X, Morel J-B (2016) Integration of decoy domains derived from protein targets of pathogen effectors into plant immune receptors is widespread. *New Phytol* 210(2):618–626.
48. Sarris PF, Cevik V, Dagdas G, Jones JDG, Krasileva KV (2016) Comparative analysis of plant immune receptor architectures uncovers host proteins likely targeted by pathogens. *BMC Biol* 14:8.
49. Tameling WIL, et al. (2010) RanGAP2 mediates nucleocytoplasmic partitioning of the NB-LRR immune receptor Rx in the Solanaceae, thereby dictating Rx function. *Plant Cell* 22(12):4176–4194.
50. Tameling WI, Baulcombe DC (2007) Physical association of the NB-LRR resistance protein Rx with a Ran GTPase-activating protein is required for extreme resistance to Potato virus X. *Plant Cell* 19(5):1682–1694.
51. Sacco MA, Mansoor S, Moffett P (2007) A RanGAP protein physically interacts with the NB-LRR protein Rx, and is required for Rx-mediated viral resistance. *Plant J* 52(1): 82–93.
52. Rairdan GJ, et al. (2008) The coiled-coil and nucleotide binding domains of the Potato Rx disease resistance protein function in pathogen recognition and signaling. *Plant Cell* 20(3):739–751.
53. Bernoux M, et al. (2008) RD19, an *Arabidopsis* cysteine protease required for RRS1-R-mediated resistance, is relocalized to the nucleus by the *Ralstonia solanacearum* PopP2 effector. *Plant Cell* 20(8):2252–2264.
54. Heidrich K, et al. (2011) *Arabidopsis* EDS1 connects pathogen effector recognition to cell compartment-specific immune responses. *Science* 334(6061):1401–1404.
55. Gietz RD, Woods RA (2002) Transformation of yeast by lithium acetate/single-stranded carrier DNA/polyethylene glycol method. *Methods Enzymol* 350:87–96.
56. Kushnirov VV (2000) Rapid and reliable protein extraction from yeast. *Yeast* 16(9): 857–860.
57. Richardson T, Thistleton J, Higgins TJ, Howitt C, Ayliffe M (2014) Efficient *Agrobacterium* transformation of elite wheat germplasm without selection. *Plant Cell Tissue Organ Cult* 119(3):647–659.
58. Shan Q, et al. (2013) Targeted genome modification of crop plants using a CRISPR-Cas system. *Nat Biotechnol* 31(8):686–688.
59. Larkin MA, et al. (2007) Clustal W and Clustal X version 2.0. *Bioinformatics* 23(21): 2947–2948.

Supporting Information

Cesari et al. 10.1073/pnas.1605483113

SI Methods

Plant Growth Conditions and Infection Assay Conditions. *Nicotiana benthamiana* plants and wheat plants were grown in a growth chamber at 23 °C with a 16-h light period. Spores derived from *Pgt* strain 98-1,2,3,5,6 were spray-inoculated on plants at the two-leaf stage, and symptoms were scored 13 d after inoculation.

Constructs. All PCR products used for cloning were generated using Phusion High-Fidelity DNA Polymerase (Thermo Fisher) and the primers listed in Table S2. Details of constructs are given in Table S3. For yeast two-hybrid assays, the $MLA10_{1–160}$, $MLA10_{1–225}$, $Sr50_{1–163}$, and $Sr50_{1–228}$ PCR products (Table S3) were cloned into pGBKT7-BD and pGADT7-AD (Clontech) using EcoR1 and Xho1 restriction sites. The AD:$RGA5_{1–228}$, BD:$RGA5_{1–228}$, BD:L6-TIR, and AD:L6-TIR constructs are described elsewhere (7, 17).

For stable wheat transformation, the genomic *Sr33* sequence including promoter and genomic gene sequence but excluding the stop codon was amplified with flanking Not1 and Apa1 restriction sites (Not1_*pSr33::Sr33*_Apa1). The *YFPv*, *YFPv:NLS*, *YFPv:NES*, *YFPv:nls*, and *YFPv:nes* fragments were amplified with flanking Apa1 and EcoR1 restriction sites. The Sr33 terminator was amplified with flanking EcoR1 and BamH1 restriction sites (EcoR1_*terSr33*_BamH1). All fragments were ligated in the binary vector pVecNeo to create the *pSr33::Sr33:YFPv*, *pSr33::Sr33:YFPv:NLS*, *pSr33::Sr33:YFPv:nls*, *pSr33::Sr33:YFPv:NES*, and *pSr33::Sr33:YFPv:nes* constructs (Table S3). To generate the *pSr33::YFPv* construct, the *Sr33* promoter sequence was PCR amplified with flanking Not1 and Apa1 sites (Not1_*pSr33*_Apa1), and this fragment was ligated in pVecNeo together with Apa1_*YFPv*_EcoR1 and EcoR1_*terSr33*_BamH1 (Table S3).

Construction of the *pSr33::Sr33* and *pSr50::Sr50* genomic constructs in pVecNeo used for transient assay in *N. benthamiana* is described elsewhere (10, 11). To generate the *pSr50::Sr50:YFPv* construct, the sequence of the YFPv was cloned upstream Sr50 terminator sequence as described in Table S3.

For other transient expression experiments in *N. benthamiana*, plasmids were generated by Gateway technology (Life Technologies) or QuikChange Lightning technology (Agilent Technologies) following the manufacturers' instructions. $MLA10_{1–160}$, $MLA10_{1–120}$, $MLA10_{1–225}$, $Sr33_{1–160}$, $Sr33_{1–120}$, $Sr33_{1–225}$, *Sr33* (full-length cDNA), $Sr50_{1–163}$, $Sr50_{1–123}$, $Sr50_{1–228}$, and *Sr50* (full-length cDNA) PCR products flanked by *attB* sites were recombined into the pDONR207 vector (Life Technologies) via a BP reaction to create corresponding entry clones (Table S3). To create point mutations in the Sr33 $CC_{1–160}$ domain or full-length protein, site-directed mutagenesis was performed on the pDONR207_$Sr33_{1–160}$ and pDONR207_Sr33 full-length cDNA entry vectors (Table S3), generating the following point mutations in both the $CC_{1–160}$ sequence and the full-length Sr33: A122E/I123E, I126E, L130E, V133E/A134E, R136A/R137A/D138A/R139A/N140A/K141A (RRDRNK/6A), and F142E. Following BP cloning or QuikChange mutagenesis, appropriate LR reactions were performed to generate the fusion constructs in the binary vectors pBIN19-35S::GTW:CFP, pBIN19-35S::YFP:GTW, pBIN19-35S::GTW:3HA, pAM-PAT-35s::GTW:YFP:NLS, pAM-PAT-35s::GTW:YFP:nls, pXCSG-35s::GTW:YFP:NES, or pXCSG-35s::GTW:YFP:nes (Table S3). The *RGA4:HA*, *RGA4:CFP*, $rga4_{TYG/MHD}$*:HA*, $rga4_{TYG/MHD}$*:CFP*, and $RGA4_{1–171}$*:CFP* constructs are described elsewhere (16, 17).

To create the pAM-PAT-35s::GTW:YFP:NLS and pAM-PAT-35s::GTW:YFP:nls vectors, a functional NLS from SV40 (PKKKRKVG) and a nonfunctional nls (PKTKRKVG) (18) were introduced in the pAM-PAT-35s-GWY-YFPv vector (53) at the C-terminal end of the YFPv. YFPv-NLS/nls fragments were PCR amplified using a forward primer containing a 3′ Sma1 site and a reverse primer containing a 5′ Xba1 site as well as the NLS or nls sequence. Corresponding PCR products were ligated into pAM-PAT-35s-GWY-YFPv cut with Sma1/Xba1 to replace the original YFPv by YFPv-NLS/nls fusions. The binary vectors pBIN19-35S::GTW:CFP and pBIN19-35S::GTW:3HA were kindly provided by Susana Rivas, Laboratory of Plant–Microbe Interactions, Toulouse, France. The pAM-PAT–derived binary vectors pXCSG-35s::GTW:YFP:NES and pXCSG-35s::GTW:YFP:nes are described elsewhere (54).

Yeast Two-Hybrid Analysis. All experiments were performed in *Saccharomyces cerevisiae* reporter strain Hf7c. Yeast transformation was performed as described (55) with cotransformants selected on synthetic defined (SD) medium lacking leucine and tryptophan (−LT). The interaction analysis was performed on medium lacking leucine, tryptophan, and histidine (−LTH) with yeast grown at 30 °C for 4 d.

Transient Protein Expression in *N. benthamiana*. For *N. benthamiana* leaf transformations, pBIN19-derived vector constructs were transformed into *Agrobacterium tumefaciens* strain GV3101_pMP90, and the pAM-PAT vector constructs were transformed into GV3103. Bacterial strains were grown in Luria–Bertani liquid medium containing 50 mg/mL rifampicin, 15 mg/mL gentamycin, and 25 mg/mL kanamycin (and 25 mg/mL of carbenicillin for pAM-PAT vectors) at 28 °C for 24 h. Bacteria were harvested by centrifugation, resuspended in infiltration medium [10 mM MES (pH 5.6), 10 mM MgCl2, and 150 μM acetosyringone] to an OD_{600} ranging from 0.5 to 1, and incubated for 2 h at room temperature before leaf infiltration. For each independent infiltration experiment, each construct was infiltrated on three leaves from three or four individual plants. The infiltrated plants were incubated in growth chambers under controlled conditions for all following assays. For documentation of cell death, leaves were photographed 2–5 d after infiltration.

Protein Extraction, Immunoblot, and Coimmunoprecipitation. Protein extraction from *N. benthamiana* leaves and coimmunoprecipitation experiments were performed as described (16). Total yeast protein was extracted as described (56). For immunoblotting analysis, proteins were separated by SDS/PAGE and transferred to a nitrocellulose membrane (Pall). Membranes were blocked in 5% skimmed milk and probed with anti-HA (Roche anti-HA 12CA5 or Roche anti–HA-HRP 3F10), anti-GFP (Roche), or anti-Myc mouse monoclonal antibodies (Roche), followed, if required, by goat anti-mouse antibodies conjugated with HRP (Pierce). Labeling was detected using the SuperSignal West Femto chemiluminescence kit (Pierce). Membranes were stained with Ponceau S to confirm equal loading.

Wheat Transformation. All derived binary vectors used for stable transformation (Table S3) were introduced into the stem rust-susceptible wheat cultivar Fielder by *A. tumefaciens*-mediated transformation as described (57). At least 12 independent T0 lines were generated for each construct. Six T0 lines per construct were chosen for analysis of stem rust resistance in the T1 generation (Table S1). For the stem rust-infection assays shown in Fig. 4, the following T1 lines were used: PC16-5 and PC16-6 (Sr33:YFPv), PC24-1 and PC24-2 (Sr33:YFPv:NES), PC26-2 and PC26-5 (Sr33:YFPv:nes), PC17-1 and PC17-2 (Sr33:YFPv:NLS), and PC19-4 and PC19-4 (Sr33:YFPv:nls).

Protoplast Isolation. A total of eight T1 seedlings from two independent transgenic lines per construct were grown under a 16-h light period at 23 °C in a growth room for 10–14 d. Protoplasts were isolated as described (58), with slight modifications. Wheat leaves were cut into 1-mm strips and were vacuum-infiltrated for 1 h at 20 mmHg in SD solution [1.5% cellulase RS, 0.3% macerozyme R10, 0.5 M mannitol, 10 mM MES (pH 5.7) with KOH, 10 mM CaCl2, 20 mM KCl, and 0.1% BSA]. Leaves were further digested for ∼10 h with gentle shaking (40 rpm). The solution was filtered through a 40-μm nylon mesh. Protoplasts were collected after centrifugation at 80 × *g* for 3 min and were washed twice with ice-cold SE solution [0.5 M mannitol, 20 mM KCl, and 4 mM MES (pH 5.7) with KOH]. Protoplasts were kept at room temperature before observations.

Confocal Microscopy. *N. benthamiana* epidermal cells were observed 20 h after agro-infiltration under a Leica TCS SP8 confocal microscope. Samples were mounted in perfluorodecalin, and specific YFP fluorescence was detected using the following spectral settings: excitation, 488 nm; detection, 515–545 nm. Autofluorescence of the chloroplasts was detected at 670–730 nm. All images were acquired using a Leica HC PL APO 63×/1.20 W CORR CS2 lens. Wheat cell images were acquired using the Online Fingerprinting mode of Zen 2012 software on a Zeiss 780 confocal microscope using a LD 40× 1.1W lens. Reference spectra for Online Fingerprinting were derived from 14-channel (517–641 nm) Lambda mode data. The YFP spectra derived from samples were compared with manufacturers' data to confirm their identity. The validity of these spectra was checked periodically on experimental samples by Spectral Unmixing of Lambda mode data, thereby confirming that the residuals channel, representing fluorescence emission from uncharacterized sources, was consistently of low intensity.

Accession Numbers. Sequence data from this article can be found in the GenBank database under the following accession numbers: *Sr33* gene and complete CDS (KF031291.1), Sr33 protein (AGQ17382.1), *Sr50* gene and complete CDS (KT725812.1), Sr50 protein (ALO61074.1), *MLA10* gene and complete CDS (AY266445.1), MLA10 protein (AAQ55541.1), *RGA4* (AB604622.1), and *RGA5* (AB604627.1).

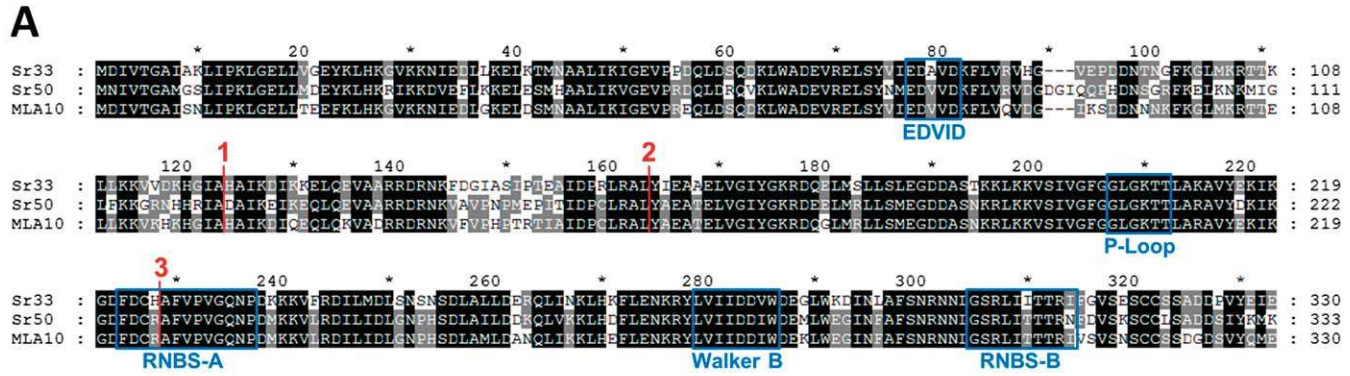

Fig. S1. Short 1–120 CC domains of MLA10, Sr33, and Sr50 are truncated. (*A*) Protein sequences were aligned using ClustalX (59) and visualized with GeneDoc (www.nrbsc.org/gfx/genedoc/ebinet.htm). Domains equivalent to MLA10 1–120, 1–160, and 1–225 are indicated by the red numbers 1, 2, and 3, respectively. (*B*) The probability that a residue in a protein is part of a CC structure was assessed by comparing its flanking sequences with sequences of known CC proteins using the CC prediction tool (15). Predictions were made using 14-, 21-, and 28-residue windows.

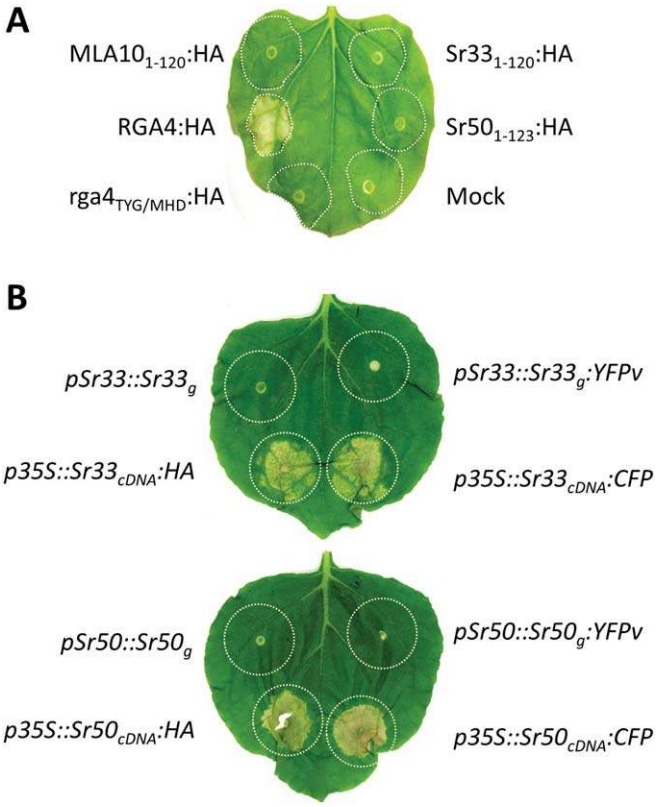

Fig. S2. Cell-death assays in *N. benthamiana*. (*A*) The MLA10 CC_{1-120}, Sr33 CC_{1-120}, and Sr50 CC_{1-123} domains fused to HA were transiently expressed in *N. benthamiana* leaves. The autoactive RGA4:HA construct was used as a positive control, and the inactive rga4$_{TYG/MHD}$:HA and a mock inoculation were used as negative controls. Cell death was visualized 4 d after infiltration. Equivalent results were obtained in three independent experiments. (*B*) The indicated *Sr33* and *Sr50* genomic constructs (including their native promoter sequences) or cDNA sequences (under the control of the *35S* promoter) were transiently expressed in *N. benthamiana* leaves by *Agrobacterium*-mediated transformation. Cell death was visualized 4 d after infiltration. Equivalent results were obtained in three independent experiments.

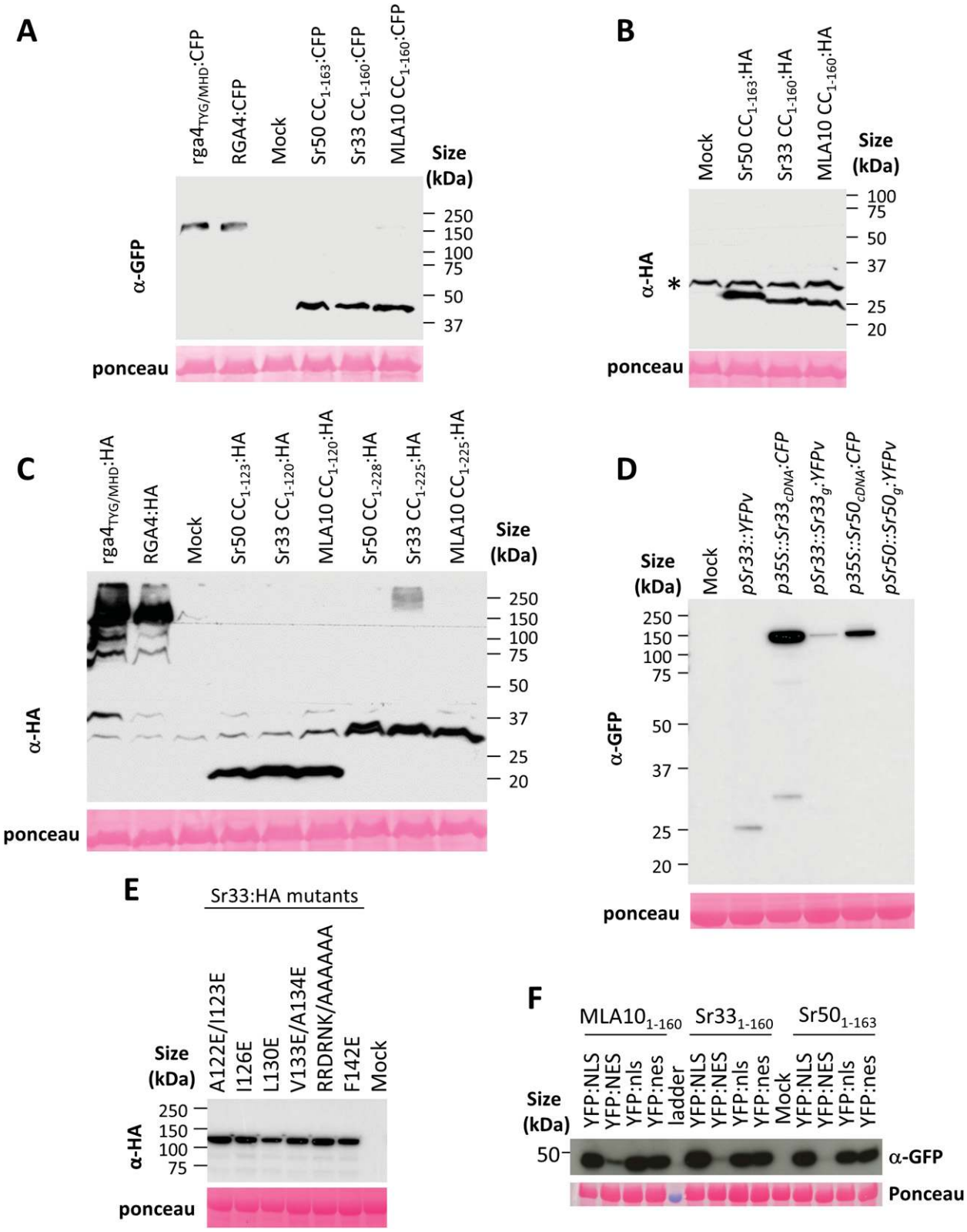

Fig. S3. (*A–F*) Immunoblotting showing expression of HA-, CFP-, or YFP-fused proteins. The indicated proteins were extracted from transiently transformed *N. benthamiana* leaves 24 h after infiltration and were analyzed by immunoblotting with anti-GFP or anti-HA antibodies. Ponceau staining of the large RuBisCO subunit was used to verify equal protein loading. An asterisk marks unspecific background.

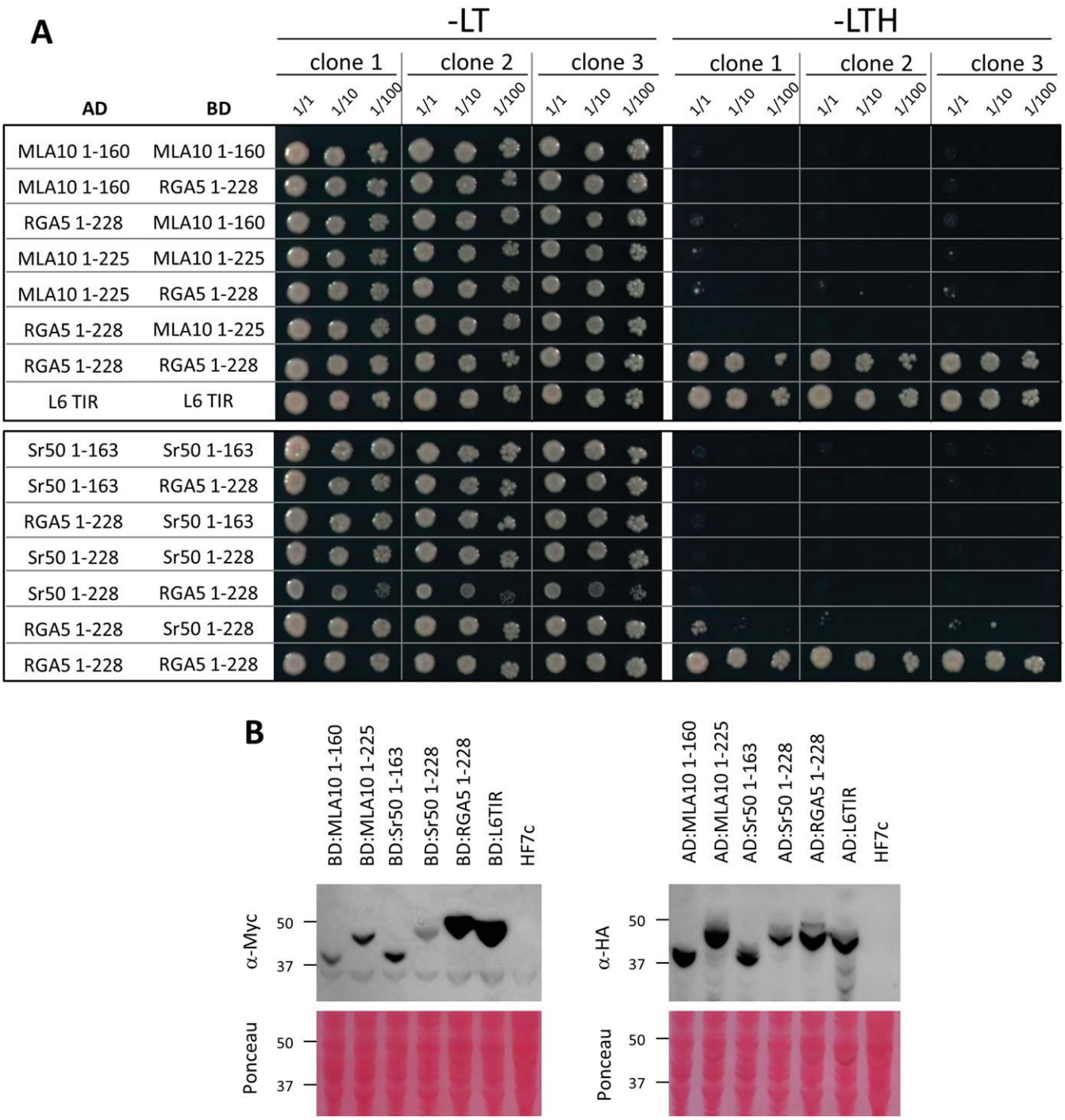

Fig. S4. The CC domains of MLA10 and Sr50 do not self-associate in yeast. (*A*) The yeast strain HF7c was cotransformed with the specified constructs, and self-interaction of MLA10 and Sr50 CC domain fragments (BD:MLA10$_{1–160}$/AD:MLA10$_{1–160}$, BD:MLA10$_{1–225}$/AD:MLA10$_{1–225}$, BD:Sr50$_{1–163}$/AD:Sr50$_{1–163}$, BD:Sr50$_{1–228}$/Ad:Sr50$_{1–228}$, and BD:Sr50$_{1–128}$/AD:Sr50$_{1–128}$) was assayed by yeast two-hybrid assay. AD:RGA5$_{1–228}$, BD:RGA5$_{1–228}$, AD:L6-TIR, and BD:L6-TIR constructs were used as controls. Cultures of cotransformed yeast clones were adjusted to an OD of 0.2, and three dilutions (1/1, 1/10, 1/100) were spotted on synthetic –LTH medium (–Trp/–Leu/–His) to assay for interactions and on synthetic double-dropout –LT medium (–Trp/–Leu) to monitor proper growth. Photographs were taken after 4 d of growth. (*B*) Myc- or HA-tagged proteins were extracted from yeasts and detected by immunoblotting using anti-Myc or anti-HA antibodies, respectively.

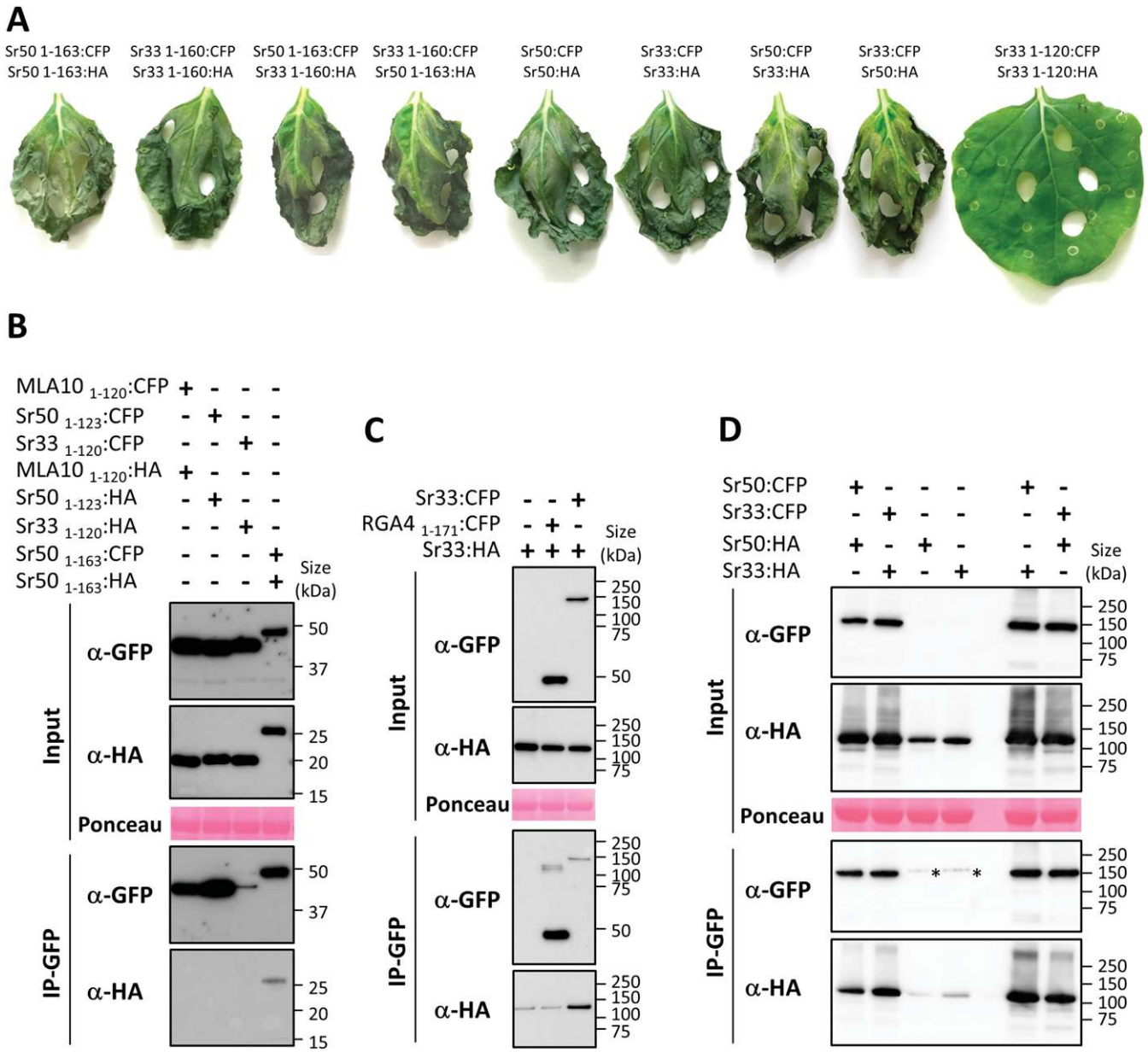

Fig. S5. Cell-death and *in planta* coimmunoprecipitation assays. (*A*) The indicated combinations of constructs fused to either the CFP or the HA tag were transiently expressed in *N. benthamiana* leaves. Samples were collected for coimmunoprecipitation assays 24 h after infiltration, and pictures were taken 3 d after infiltration. (*B*) The truncated CC domains of MLA10, Sr33, and Sr50 do not self-associate *in planta*. Coimmunoprecipitation was performed as described in Fig. 2. The Sr50 $CC_{1–160}$ positive control was included in the experiment. (*C*) The full-length Sr33 protein self-associates *in planta*. Coimmunoprecipitation was performed as described in Fig. 2. An additional control was included to test Sr33-unspecific binding to the GFP-trap_M beads. (*D*) Full-length Sr33 and Sr50 homo- and hetero-associate *in planta*. Coimmunoprecipitation was performed as described in Fig. 2. A control was included to test Sr33- and Sr50-unspecific binding to the GFP-trap_M beads.

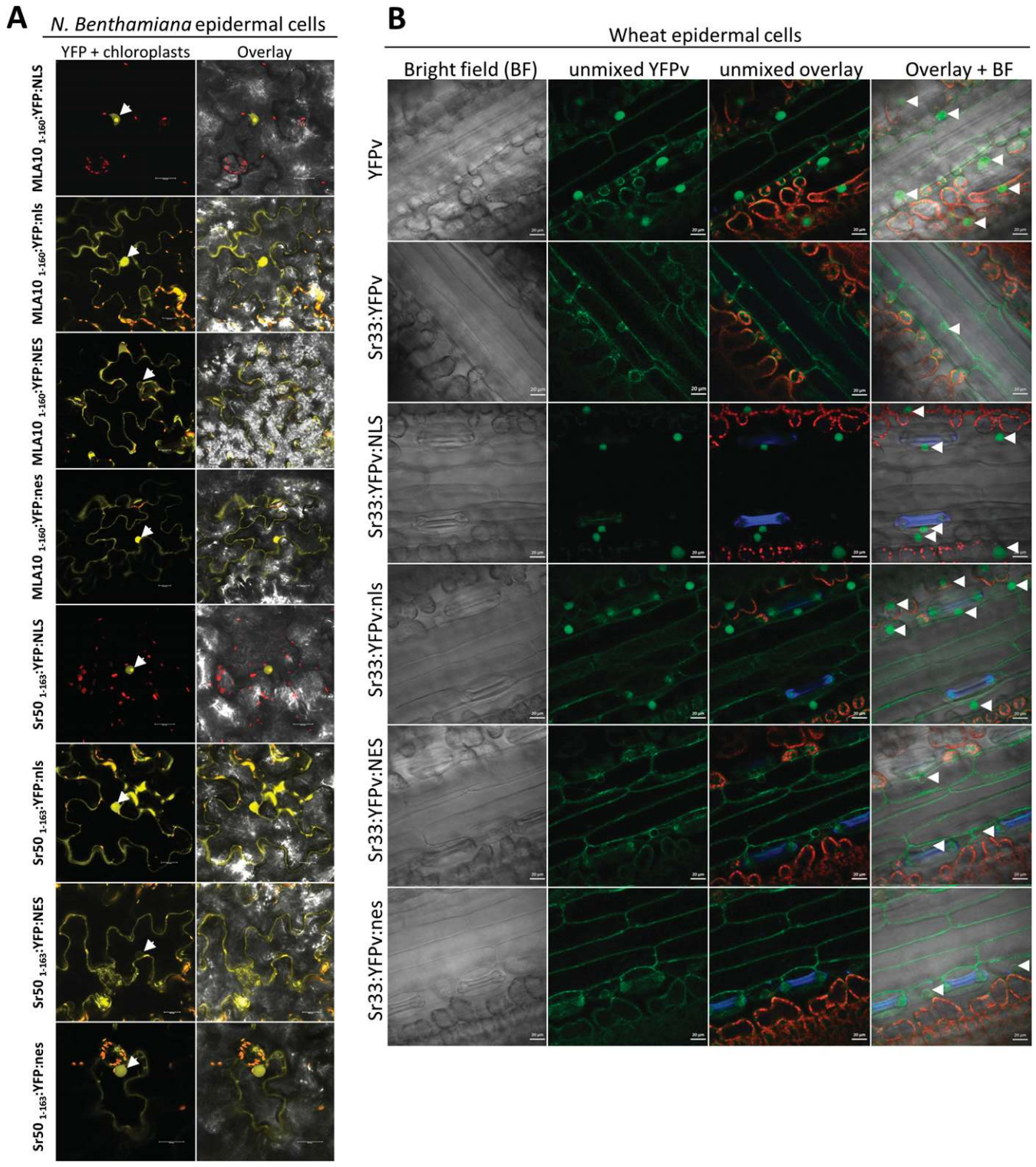

Fig. S6. Confocal imaging in *N. benthamiana* and wheat epidermal cells. (*A*) CC domains fused to YFP:NLS, YFP:nls, YFP:NES, or YFP:nes were transiently expressed in *N. benthamiana*. Confocal images were taken 20 h after infiltration. Arrows indicate nuclei. (Scale bars, 20 μm.) (*B*) Confocal images showing localization of Sr33 fused to the YFPv, YFPv:NLS, YFPv:nls, YFPv:NES, or YFPv:nes in transgenic wheat leaf epidermal cells were taken on 10- to14-d-old T1 plants. YFPv fluorescence appears in green; stomatal and chloroplastic autofluorescence emissions are shown in blue and red, respectively. White arrowheads mark nuclei. (Scale bars, 20 μm.)

Table S1. Segregation of stem rust resistance in transgenic wheat lines

Transformed construct	Independent transgenic lines tested for stem rust resistance	No. of tested independent transgenic lines showing resistance	No. of resistant/total plants for each line tested
pSr33::Sr33:YFPv:NLS	PC17-1	0	0/≥20
	PC17-2		0/≥20
	PC17-3		0/≥20
	PC17-4		0/≥20
	PC17-5		0/≥20
	PC17-7		0/≥20
pSr33::Sr33:YFPv:nls	PC19-1	6	16/20
	PC19-2		15/15
	PC19-3		18/18
	PC19-4		23/24
	PC19-5		13/19
	PC19-6		12/17
pSr33::Sr33:YFPv:NES	PC24-1	6	21/23
	PC24-2		30/32
	PC24-3		20/22
	PC24-4		26/28
	PC24-5		16/22
	PC24-6		20/20
pSr33::Sr33:YFPv:nes	PC26-1	6	20/20
	PC26-2		14/16
	PC26-4		18/18
	PC26-5		16/18
	PC26-6		6/9
	PC26-7		12/12
pSr33::Sr33:YFPv	PC16-1	3	0/≥20
	PC16-2		19/25
	PC16-3		0/≥20
	PC16-4		0/≥20
	PC16-5		18/20
	PC16-6		11/15
pSr33::YFPv	PC25-1	0	0/≥20
	PC25-2		0/≥20
	PC25-3		0/≥20
	PC25-4		0/≥20
	PC25-5		0/≥20
	PC25-6		0/≥20

Table S2. Primers used in this study

Primer name	Primer sequence 5′–3′
oCS184	GGGGACAAGTTTGTACAAAAAAGCAGGCTTAATG AATATTGTCACGGGGGCC
oCS187	GGGGACCACTTTGTACAAGAAAGCTGGGTCCAAAGCTCGAAGACAAGGATCGA
oCS195	GGGGACAAGTTTGTACAAAAAAGCAGGCTTAATGGATATTGTCACCGGTGCC
oCS197	GGGGACCACTTTGTACAAGAAAGCTGGGTCCAAAGCTCGAAGGCAAGGGTC
oCS204	GGGGACAAGTTTGTACAAAAAAGCAGGCTTAATGGATATTGTCACGGGTGCC
oCS206	GGGGACCACTTTGTACAAGAAAGCTGGGTCTAGAGCACGGAGACGAGGATCA
oCS211	GGGGACCACTTTGTACAAGAAAGCTGGGTCAGCTATCCCATGCTTATGCTTGAC
oCS212	GGGGACCACTTTGTACAAGAAAGCTGGGTCAGCTATTCCATGCTTATCCACGAC
oCS213	GGGGACCACTTTGTACAAGAAAGCTGGGTCAGCTATGCGATGGTGATTCCTG
oCS214	GGGGACCACTTTGTACAAGAAAGCTGGGTCCCGACAATCGAAATCACCTTTAATC
oCS215	GGGGACCACTTTGTACAAGAAAGCTGGGTCGTGACAATCAAAATCACCTTTAATC
oCS216	GGGGACCACTTTGTACAAGAAAGCTGGGTCCCGACAATCAAAATCACCTTTAATC
oCS317	GGATAAGCATGGAATAGCTCACGAGGAGAAGGACATCAAGAAGGAACTCCA
oCS318	TGGAGTTCCTTCTTGATGTCCTTCTCCTCGTGAGCTATTCCATGCTTATCC
oCS320	GCTCACGCGATCAAGGACGAGAAGAAGGAACTCCAGGAG
oCS321	CTCCTGGAGTTCCTTCTTCTCGTCCTTGATCGCGTGAGC
oCS322	GCGATCAAGGACATCAAGAAGGAAGAGCAGGAGGTGGCTG
oCS323	CAGCCACCTCCTGCTCTTCCTTCTTGATGTCCTTGATCGC
oCS324	AGGAACTCCAGGAGGAGGAGGCTAGGCGTGACAGG
oCS325	CCTGTCACGCCTAGCCTCCTCCTCCTGGAGTTCCT
oCS326	ACATCAAGAAGGAACTCCAGGAGGTGGCTGCTGCGGCTGCCGCGGCCGCGTTCGATGGTATTGCTTCTATTCCTACTGAAG
oCS327	CTTCAGTAGGAATAGAAGCAATACCATCGAACGCGGCCGCGGCAGCCGCAGCAGCCACCTCCTGGAGTTCCTTCTTGATGT
oCS328	GCTAGGCGTGACAGGAACAAGGAGGATGGTATTGCTTCTATTCCT
oCS329	AGGAATAGAAGCAATACCATCCTCCTTGTTCCTGTCACGCCTAGC
Sr50F EcoRI	GCATAGAATTCATGAATATTGTCACGGGGGCCATG
Sr50163R XhoI	GCTATCTCGAGTCACAAAGCTCGAAGACAAGGATCGATAG
Sr50228R XhoI	GCTATCTCGAGTCACCGACAATCAAAATCACCTTTAATCTTG
MLA10F EcoRI	GCATAGAATTCATGGATATTGTCACCGGTGCCATTTC
MLA10160R XhoI	GCTATCTCGAGTCACAAAGCTCGAAGGCAAGGGTCA
MLA10225R XhoI	CGTATCTCGAGTCACCGACAATCGAAATCACCTTTAATCTT
SmaI ccdB Fwd	CCCCCCGGGCGACGGATGGTGATCCCCCT
Xba1 NLS-YFPrev	GGGTCTAGAGTCAACCTCCTACTTTTCGCTTCTTCTTTGGCTTGTACAGCTCGTCCATGCCGA
Xba1 nls-YFPrev	GGGTCTAGAGTCAACCTCCTACCTTTCGCTTAGTCTTTGGCTTGTACAGCTCGTCCATGCCGA
Sr33 Prom NotI-F	GCATAGCGGCCGCTTCAAGATGTCAAATTTTAAAAGGGCTATT
Sr33 PromR-ApaI	CGTATGGGCCCGAGAGCTCTCTTGATCAATCAGCTGAAAC
Sr33 full length ApaI-R	GCTATGGGCCCCTCTGCGTCAGAAATCGGTCCTC
Venus ApaI Link-F	GCATAGGGCCCGGCGGTAGCGGCGGAGTGAGCAAGGGCGAGGAGCTGTT
Venus-w-NLS-R EcoRI	ATGAATTCTTAACCACCGACCTTTCTCTTCTTTTTTGGTTGCTTGTACAGCTCGTCCATGCCGAG
Venus-m-nls-R EcoRI	ATGAATTCTTAACCACCAACTTTACGAGTTTTTTTAGGTTGCTTGTACAGCTCGTCCATGCCGAG
Venus-m-nes-R EcoRI	ATGAATTCTTATTTATTAGCATCAGCACCAGCAGCTTTAAGAGCAAGTTCATTCTTGTACAGCTCGTCCATGCCGAG
Venus-NES2- EcoRI	ATGAATTCTCACTTGTTGATGTCGAGGCCGGCGAGCTTGAGGGCGAGCTCGTTCTTGTACAGCTCGTCCATGCCGAG
Sr33 Term EcoRI-F	GCATAGAATTCCTGACGTTGCTTCAGGTGTGCTCTC
Sr33 Term BamHI-R	TATGCGGATCCACCTCATTAGGAGGGAGCTGGCG
Venus-full length-R EcoRI	ATGAATTCTTACTTGTACAGCTCGTCCATGCCGA
Sr33 attB1-F	GGGGACAAGTTTGTACAAAAAAGCAGGCTTAATGGATATTGTCACGGGTGC
Sr33 attB2-R	GGGGACCACTTTGTACAAGAAAGCTGGGTCCTCTGCGTCAGAAATCGGTC
Sr50 attB1-F	GGGGACAAGTTTGTACAAAAAAGCAGGCTTAATGAATATTGTCACGGGGGC
Sr50 attB2-R	GGGGACCACTTTGTACAAGAAAGCTGGGTCGTTCTCCTCACACAAATCATCATCT
Sr33 genotyping-F	GTCCCTTCGCCGTCTGCT
Sr33 genotyping-R	GGTCCTCCAACCGGGTAAC
Sr50 F1	TCCCTTCGGCATGATGTCT
Sr50 R1	AAGGGCCCAACCCGGGGTTCTCCTCACACAAATCATCATCA
Sr50 F2	AACCCGGGAAAGTTTAAACTTTATGATGTAGAGGACTCACAGTGAAT
Sr50 R2	AAGGGCCCTGGGCGTGACTGTGCTG
Venus F	AACCCGGGGTGAGCAAGGGCGAGGAG
Venus R	AAAGTTTAAACTTACTTGTACAGCTCGTCCATGC

Table S3. Plasmids generated in this study

Use	Construct	Plasmid name	Insert or PCR product	Primers	Template	Plasmid backbone	Cloning method	Source
Entry clones for *N. benthamiana* assays	$MLA10_{1–160}$	pSC260	$MLA10_{1–160}$ (without stop)	oCS195/197	Plasmid (cDNA) from Paul Schulze-Lefert* (13)	pDONR207	BP Gateway (Life Technologies)	–
	$MLA10_{1–120}$	pSC323	$MLA10_{1–120}$ (without stop)	oCS195/211	Plasmid (cDNA) from Paul Schulze-Lefert (13)	pDONR207	BP Gateway	–
	$MLA10_{1–225}$	pSC324	$MLA10_{1–225}$ (without stop)	oCS195/214	Plasmid (cDNA) from Paul Schulze-Lefert (13)	pDONR207	BP Gateway	–
	$Sr33_{1–160}$	pSC298	$Sr33_{1–160}$ (without stop)	oCS204/206	Plasmid (cDNA) from S.P. (10)	pDONR207	BP Gateway	–
	$Sr33_{1–120}$	pSC325	$Sr33_{1–120}$ (without stop)	oCS204/212	Plasmid (cDNA) from S.P. (10)	pDONR207	BP Gateway	–
	$Sr33_{1–225}$	pSC326	$Sr33_{1–225}$ (without stop)	oCS204/215	Plasmid (cDNA) from S.P. (10)	pDONR207	BP Gateway	–
	$Sr33_{1–160}$ A122E/I123E	pSC437	$Sr33_{1–160}$ A122E/I123E (without stop)	oCS317/318	pSC298	pDONR207	QuikChange Lightning (Agilent Technologies)	–
	$Sr33_{1–160}$ I126E	pSC438	$Sr33_{1–160}$ I126E (without stop)	oCS320/321	pSC298	pDONR207	QuikChange Lightning	–
	$Sr33_{1–160}$ L130E	pSC439	$Sr33_{1–160}$ L130E (without stop)	oCS322/323	pSC298	pDONR207	QuikChange Lightning	–
	$Sr33_{1–160}$ V133E/A134E	pSC440	$Sr33_{1–160}$ V133E/A134E (without stop)	oCS324/325	pSC298	pDONR207	QuikChange Lightning	–
	$Sr33_{1–160}$ RRDRNK/AAAAAAA	pSC441	$Sr33_{1–160}$ RRDRNK/AAAAAAA (without stop)	oCS326/327	pSC298	pDONR207	QuikChange Lightning	–
	$Sr33_{1–160}$ F142E	pSC442	$Sr33_{1–160}$ F142E (without stop)	oCS328/329	pSC298	pDONR207	QuikChange Lightning	–
	Sr33 full-length	Sr33 full length entry (C.C.)	Sr33 full-length (without stop)	Sr33 attB1-F/Sr33 attB2-R	pGBCT-Sr33 (cDNA) from S.P. (10)	pDONR207	BP Gateway	–
	Sr33 full-length A122E/I123E	pSC443	Sr33 full-length A122E/I123E (without stop)	oCS317/318	C.C. Sr33 full-length entry	pDONR207	QuikChange Lightning	–
	Sr33 full-length I126E	pSC444	Sr33 full-length I126E (without stop)	oCS320/321	C.C. Sr33 full-length entry	pDONR207	QuikChange Lightning	–
	Sr33 full-length L130E	pSC445	Sr33 full-length L130E (without stop)	oCS322/323	C.C. Sr33 full-length entry	pDONR207	QuikChange Lightning	–
	Sr33 full-length V133E/A134E	pSC446	Sr33 full-length V133E/A134E (without stop)	oCS324/325	C.C. Sr33 full-length entry	pDONR207	QuikChange Lightning	–
	Sr33 full-length RRDRNK/AAAAAAA	pSC447	Sr33 full-length RRDRNK/AAAAAAA (without stop)	oCS326/327	C.C. Sr33 full-length entry	pDONR207	QuikChange Lightning	–
	Sr33 full-length F142E	pSC448	Sr33 full-length F142E (without stop)	oCS328/329	C.C. Sr33 full-length entry	pDONR207	QuikChange Lightning	–
	$Sr50_{1–163}$	pSC262	$Sr50_{1–163}$ (without stop)	oCS184/187	Plasmid (Sr50 genomic) from R.M. (11)	pDONR207	BP Gateway	–
	$Sr50_{1–123}$	pSC327	$Sr50_{1–123}$ (without stop)	oCS184/213	Plasmid (Sr50 genomic) from R.M. (11)	pDONR207	BP Gateway	–
	$Sr50_{1–228}$	pSC328	$Sr50_{1–228}$ (without stop)	oCS184/216	Plasmid (Sr50 genomic) from R.M. (11)	pDONR207	BP Gateway	–
	Sr50 full length	Sr50 full length entry (C.C.)	Sr50 full length (without stop)	Sr50 attB1-F/Sr50 attB2-R	pGEMT-Sr50 (cDNA) from R.M. (11)	pDONR207	BP Gateway	–

Table S3. Cont.

Use	Construct	Plasmid name	Insert or PCR product	Primers	Template	Plasmid backbone	Cloning method	Source
Cell-death assays, co-IPs, and confocal microscopy in *N. benthamiana*	RGA4:HA	pSC061	RGA4 (cDNA)	–	–	–	–	(46)
	RGA4:CFP	pSC081	RGA4 (cDNA)	–	–	–	–	(46)
	$RGA4_{MHD}$:HA	pSC285	$RGA4_{MHD}$	–	–	–	–	(46)
	$RGA4_{MHD}$:CFP	pSC306	$RGA4_{MHD}$	–	–	–	–	(46)
	$RGA4_{1–171}$:CFP	pSC167	$RGA4_{1–171}$	–	–	–	–	(46)
	$MLA10_{1–160}$:HA	pSC278	$MLA10_{1–160}$	–	pSC260	pBin19-35s::GTW:HA	LR Gateway (Life Technologies)	–
	$MLA10_{1–160}$:CFP	pSC302	$MLA10_{1–160}$	–	pSC260	pBin19-35s::GTW:CFP	LR Gateway	–
	$MLA10_{1–160}$:YFP:NLS	pSC311	$MLA10_{1–160}$	–	pSC260	pAM-PAT-35s::GTW:YFP:NLS	LR Gateway	–
	$MLA10_{1–160}$:YFP:nls	pSC313	$MLA10_{1–160}$	–	pSC260	pAM-PAT-35s::GTW:YFP:nls	LR Gateway	–
	$MLA10_{1–160}$:YFP:NES	pSC312	$MLA10_{1–160}$	–	pSC260	pXCSG-35s::GTW:YFP:NES (54)	LR Gateway	–
	$MLA10_{1–160}$:YFP:nes	pSC314	$MLA10_{1–160}$	–	pSC260	pXCSG-35s::GTW:YFP:nes (54)	LR Gateway	–
	$MLA10_{1–225}$:HA	pSC338	$MLA10_{1–225}$	–	pSC324	pBin19-35s::GTW:HA	LR Gateway	–
	$MLA10_{1–120}$:HA	pSC337	$MLA10_{1–120}$	–	pSC323	pBin19-35s::GTW:HA	LR Gateway	–
	$MLA10_{1–120}$:CFP	pSC343	$MLA10_{1–120}$	–	pSC323	pBin19-35s::GTW:CFP	LR Gateway	–
	$Sr33_{1–160}$:HA	pSC300	$Sr33_{1–160}$	–	pSC298	pBin19-35s::GTW:HA	LR Gateway	–
	$Sr33_{1–160}$:CFP	pSC301	$Sr33_{1–160}$	–	pSC298	pBin19-35s::GTW:CFP	LR Gateway	–
	$Sr33_{1–160}$:YFP:NLS	pSC315	$Sr33_{1–160}$	–	pSC298	pAM-PAT-35s::GTW:YFP:NLS	LR Gateway	–
	$Sr33_{1–160}$:YFP:nls	pSC317	$Sr33_{1–160}$	–	pSC298	pAM-PAT-35s::GTW:YFP:nls	LR Gateway	–
	$Sr33_{1–160}$:YFP:NES	pSC316	$Sr33_{1–160}$	–	pSC298	pXCSG-35s::GTW:YFP:NES (54)	LR Gateway	–
	$Sr33_{1–160}$:YFP:nes	pSC318	$Sr33_{1–160}$	–	pSC298	pXCSG-35s::GTW:YFP:nes (54)	LR Gateway	–
	$Sr33_{1–120}$:HA	pSC339	$Sr33_{1–120}$	–	pSC325	pBin19-35s::GTW:HA	LR Gateway	–
	$Sr33_{1–120}$:CFP	pSC345	$Sr33_{1–120}$	–	pSC325	pBin19-35s::GTW:CFP	LR Gateway	–
	$Sr33_{1–225}$:HA	pSC340	$Sr33_{1–225}$	–	pSC326	pBin19-35s::GTW:HA	LR Gateway	–
	$Sr33_{1–160}$ A122E/I123E:HA	pSC449	$Sr33_{1–160}$ A122E/I123E	–	pSC437	pBin19-35s::GTW:HA	LR Gateway	–
	$Sr33_{1–160}$ I126E:HA	pSC450	$Sr33_{1–160}$ I126E	–	pSC438	pBin19-35s::GTW:HA	LR Gateway	–
	$Sr33_{1–160}$ L130E:HA	pSC451	$Sr33_{1–160}$ L130E	–	pSC439	pBin19-35s::GTW:HA	LR Gateway	–
	$Sr33_{1–160}$ V133E/A134E:HA	pSC452	$Sr33_{1–160}$ V133E/A134E	–	pSC440	pBin19-35s::GTW:HA	LR Gateway	–
	$Sr33_{1–160}$ R136A/R137A/ D138A/R139A/ N140A/K141A:HA	pSC453	$Sr33_{1–160}$ R136A/R137A/ D138A/R139A/ N140A/K141A	–	pSC441	pBin19-35s::GTW:HA	LR Gateway	–
	$Sr33_{1–160}$ F142E:HA	pSC454	$Sr33_{1–160}$ F142E	–	pSC442	pBin19-35s::GTW:HA	LR Gateway	–
	$Sr33_{1–160}$ A122E/I123E:CFP	pSC455	$Sr33_{1–160}$ A122E/I123E	–	pSC437	pBin19-35s::GTW:CFP	LR Gateway	–
	$Sr33_{1–160}$ I126E:CFP	pSC456	$Sr33_{1–160}$ I126E	–	pSC438	pBin19-35s::GTW:CFP	LR Gateway	–
	$Sr33_{1–160}$ L130E:CFP	pSC457	$Sr33_{1–160}$ L130E	–	pSC439	pBin19-35s::GTW:CFP	LR Gateway	–
	$Sr33_{1–160}$ V133E/A134E:CFP	pSC458	$Sr33_{1–160}$ V133E/A134E	–	pSC440	pBin19-35s::GTW:CFP	LR Gateway	–
	$Sr33_{1–160}$ RRDRNK/ AAAAAAA:CFP	pSC459	$Sr33_{1–160}$ RRDRNK/AAAAAAA	–	pSC441	pBin19-35s::GTW:CFP	LR Gateway	–
	$Sr33_{1–160}$ F142E:CFP	pSC460	$Sr33_{1–160}$ F142E	–	pSC442	pBin19-35s::GTW:CFP	LR Gateway	–
	Sr33 full-length:HA	Sr33:HA (C.C.)	Sr33 full-length	–	C.C. Sr33 full-length entry	pBin19-35s::GTW:HA	LR Gateway	–
	Sr33 full length:CFP	Sr33:CFP (C.C.)	Sr33 full length	–	C.C. Sr33 full length entry	pBin19-35s::GTW:CFP	LR Gateway	–
	Sr33 full-length A122E/I123E:HA	pSC461	Sr33 full-length A122E/I123E	–	pSC443	pBin19-35s::GTW:HA	LR Gateway	–
	Sr33 full-length I126E:HA	pSC462	Sr33 full-length I126E	–	pSC444	pBin19-35s::GTW:HA	LR Gateway	–
	Sr33 full-length L130E:HA	pSC463	Sr33 full-length L130E	–	pSC445	pBin19-35s::GTW:HA	LR Gateway	–
	Sr33 full-length V133E/ A134E:HA	pSC464	Sr33 full-length V133E/A134E	–	pSC446	pBin19-35s::GTW:HA	LR Gateway	–

Table S3. Cont.

Use	Construct	Plasmid name	Insert or PCR product	Primers	Template	Plasmid backbone	Cloning method	Source
	Sr33 full-length RRDRNK/AAAAAAA:HA	pSC465	Sr33 full-length RRDRNK/AAAAAAA	–	pSC447	pBin19-35s::GTW:HA	LR Gateway	–
	Sr33 full-length F142E:HA	pSC466	Sr33 full-length F142E	–	pSC448	pBin19-35s::GTW:HA	LR Gateway	–
	$Sr50_{1–163}$:HA	pSC280	$Sr50_{1–163}$	–	pSC262	pBin19-35s::GTW:HA	LR Gateway	–
	$Sr50_{1–163}$:CFP	pSC303	$Sr50_{1–163}$	–	pSC262	pBin19-35s::GTW:CFP	LR Gateway	–
	$Sr50_{1–163}$:YFP:NLS	pSC319	$Sr50_{1–163}$	–	pSC262	pAM-PAT-35s::GTW:YFP:NLS	LR Gateway	–
	$Sr50_{1–163}$:YFP:nls	pSC321	$Sr50_{1–163}$	–	pSC262	pAM-PAT-35s::GTW:YFP:nls	LR Gateway	–
	$Sr50_{1–163}$:YFP:NES	pSC320	$Sr50_{1–163}$	–	pSC262	pXCSG-35s::GTW:YFP:NES (54)	LR Gateway	–
	$Sr50_{1–163}$:YFP:nes	pSC322	$Sr50_{1–163}$	–	pSC262	pXCSG-35s::GTW:YFP:nes (54)	LR Gateway	–
	$Sr50_{1–123}$:HA	pSC341	$Sr50_{1–123}$	–	pSC327	pBin19-35s::GTW:HA	LR Gateway	–
	$Sr50_{1–123}$:CFP	pSC347	$Sr50_{1–123}$	–	pSC327	pBin19-35s::GTW:CFP	LR Gateway	–
	$Sr50_{1–228}$:HA	pSC342	$Sr50_{1–228}$	–	pSC328	pBin19-35s::GTW:HA	LR Gateway	–
	Sr50 full-length:HA	Sr50:HA (C.C.)	Sr50 full-length	–	C.C. Sr50 full-length entry	pBin19-35s::GTW:HA	LR Gateway	–
	Sr50 full-length:CFP	Sr50:CFP (C.C.)	Sr50 full-length	–	C.C. Sr50 full-length entry	pBin19-35s::GTW:CFP	LR Gateway	–
Yeast two-hybrid assay	GAL4BD:cMyc:$Sr50_{1–163}$	BD:$Sr50_{1–163}$ (J.M.)	$Sr50_{1–163}$	Sr50F EcoRI/ Sr50163R XhoI	Plasmid (Sr50 cDNA) from R.M.	pGBKT7	Direct cloning (EcoRI/XbaI)	–
	GAL4AD:HA:$Sr50_{1–163}$	AD:$Sr50_{1–163}$ (J.M.)	$Sr50_{1–163}$	Sr50F EcoRI/ Sr50163R XhoI	Plasmid (Sr50 cDNA) from R.M.	pGADT7	Direct cloning (EcoRI/XbaI)	–
	GAL4BD:cMyc:$Sr50_{1–228}$	BD:$Sr50_{1–228}$ (J.M.)	$Sr50_{1–228}$	Sr50F EcoRI/ Sr50228R XhoI	Plasmid (Sr50 cDNA) from R.M.	pGBKT7	Direct cloning (EcoRI/XbaI)	–
	GAL4AD:HA:$Sr50_{1–228}$	AD:$Sr50_{1–228}$ (J.M.)	$Sr50_{1–228}$	Sr50F EcoRI/ Sr50228R XhoI	Plasmid (Sr50 cDNA) from R.M.	pGADT7	Direct cloning (EcoRI/XbaI)	–
	GAL4BD:cMyc:$MLA10_{1–160}$	BD:$MLA10_{1–160}$ (J.M.)	$MLA10_{1–160}$	MLA10F EcoRI/ MLA10160R XhoI	Plasmid (cDNA) from Paul Schulze-Lefert (13)	pGBKT7	Direct cloning (EcoRI/XbaI)	–
	GAL4AD:HA:$MLA10_{1–160}$	AD:$MLA10_{1–160}$ (J.M.)	$MLA10_{1–160}$	MLA10F EcoRI/ MLA10160R XhoI	Plasmid (cDNA) from Paul Schulze-Lefert (13)	pGADT7	Direct cloning (EcoRI/XbaI)	–
	GAL4BD:cMyc:$MLA10_{1–225}$	BD:$MLA10_{1–225}$ (J.M.)	$MLA10_{1–225}$	MLA10F EcoRI/ MLA10225R XhoI	Plasmid (cDNA) from Paul Schulze-Lefert (13)	pGBKT7	Direct cloning (EcoRI/XbaI)	–
	GAL4AD:HA:$MLA10_{1–225}$	AD:$MLA10_{1–225}$ (J.M.)	$MLA10_{1–225}$	MLA10F EcoRI/ MLA10225R XhoI	Plasmid (cDNA) from Paul Schulze-Lefert 13)	pGADT7	Direct cloning (EcoRI/XbaI)	–
	GAL4BD:cMyc:$RGA5_{1–228}$	BD:RGA5 (M.B.)	$RGA5_{1–228}$	–	–	–	–	(16)
	GAL4AD:HA:$RGA5_{1–228}$	AD:RGA5 (M.B.)	$RGA5_{1–228}$	–	–	–	–	(16)
	GAL4BD:cMyc:L6_TIR	BD:L6-TIR (M.B.)	L6-TIR	–	–	–	–	(7)
	GAL4AD:HA:L6_TIR	AD:L6-TIR (M.B.)	L6-TIR	–	–	–	–	(7)
Binary GWY vectors construction for *N. benthamiana* assays	–	pAM-PAT-35s::GTW:YFPv:NLS	Sma1-YFP-NLS-Xba1	SmaI ccdB Fwd/ Xba1 NLS-YFP rev	pAM-PAT-35s::GTW:YFPv	pAM-PAT-35s::GTW:YFPv (53)	Direct cloning (Sma1/XbaI)	–
	–	pAM-PAT-35s::GTW:YFPv:nLs	Sma1-YFP-nls-Xba1	SmaI ccdB Fwd/ Xba1 nls-YFP rev	pAM-PAT-35s::GTW:YFPv	pAM-PAT-35s::GTW:YFPv (53)	Direct cloning (Sma1/XbaI)	–
Stable wheat transformation and/or cell-death assays in *N. benthamiana*	pSr33::Sr33:YFPv:NLS:terSr33	PC17 (J.M.)	Not1-pSr33::Sr33(without stop)-Apa1	Sr33 Prom NotI-F/ Sr33 Full-length ApaI-R	plasmid (genomic DNA) from S.P. (10)	pVecNeo	Some fragments were ligated in pGEM-T easy vector (Promega) and sequentially ligated in pVecNeo (Apa1/BamH1 and Not1/Apa1)	–
			Apa1-YFPv:NLS(with stop)-EcoR1	Venus ApaI Link-F/ Venus-w-NLS-R EcoRI	pAM-PAT-35s::GTW:YFPv			–
			EcoR1-Sr33ter-BamH1	Sr33 Term EcoRI-F/ Sr33 Term BamHI-R	Plasmid (genomic DNA) from S.P. (10)			–
	pSr33::Sr33:YFPv:nls:terSr33	PC19 (J.M.)	Not1-pSr33::Sr33(without stop)-Apa1	Sr33 Prom NotI-F/ Sr33 Full-length ApaI-R	Plasmid (genomic DNA) from S.P. (10)	pVecNeo	Some fragments were ligated in pGEM-T easy vector	–

Table S3. Cont.

Use	Construct	Plasmid name	Insert or PCR product	Primers	Template	Plasmid backbone	Cloning method	Source
			Apa1-YFPv:nls(with stop)-EcoR1	Venus ApaI Link-F/ Venus-m-nls-R EcoRI	pAM-PAT-35s::GTW:YFPv		(Promega) and sequentially ligated in pVecNeo (Apa1/	–
			EcoR1-Sr33ter-BamH1	Sr33 Term EcoRI-F/ Sr33 Term BamHI-R	Plasmid (genomic DNA) from S.P. (10)		BamH1 and Not1/Apa1)	–
	pSr33::Sr33:YFPv:NES:terSr33	PC24 (J.M.)	Not1-pSr33::Sr33(without stop)-Apa1	Sr33 Prom NotI-F/ Sr33 Full-length ApaI-R	Plasmid (genomic DNA) from S.P. (10)	pVecNeo	Some fragments were ligated in pGEM-T easy vector	–
			Apa1-YFPv:NES(with stop)-EcoR1	Venus ApaI Link-F/ Venus-NES2- EcoRI	pAM-PAT-35s::GTW:YFPv		(Promega) and sequentially ligated in pVecNeo (Apa1/	–
			EcoR1-Sr33ter-BamH1	Sr33 Term EcoRI-F/ Sr33 Term BamHI-R	Plasmid (genomic DNA) from S.P. (10)		BamH1 and Not1/Apa1)	–
	pSr33::Sr33:YFPv:nes:terSr33	PC26 (J.M.)	Not1-pSr33::Sr33(without stop)-Apa1	Sr33 Prom NotI-F/ Sr33 Full-length ApaI-R	Plasmid (genomic DNA) from S.P. (10)	pVecNeo	Some fragments were ligated in pGEM-T easy vector	–
			Apa1-YFPv:nes(with stop)-EcoR1	Venus ApaI Link-F/ Venus-m-nesR EcoRI	pAM-PAT-35s::GTW:YFPv		Promega) and sequentially ligated in pVecNeo (Apa1/	–
			EcoR1-Sr33ter-BamH1	Sr33 Term EcoRI-F/ Sr33 Term BamHI-R	Plasmid (genomic DNA) from S.P. (10)		BamH1 and Not1/Apa1)	–
	pSr33::Sr33:YFPv:terSr33	PC16 (J.M.)	Not1-pSr33::Sr33(without stop)-Apa1	Sr33 Prom NotI-F/Sr33 full-length ApaI-R	Plasmid (genomic DNA) from S.P. (10)	pVecNeo	Some fragments were ligated in pGEM-T easy vector	–
			Apa1-YFPv(with stop)-EcoR1	Venus ApaI Link-F/ Venus-full-length-R EcoRI	pAM-PAT-35s::GTW:YFPv		(Promega) and sequentially ligated in pVecNeo (Apa1/ BamH1 and Not1/Apa1)	–
			EcoR1-Sr33ter-BamH1	Sr33 Term EcoRI-F/ Sr33 Term BamHI-R	Plasmid (genomic DNA) from S.P. (10)			–
	pSr33::YFPv:terSr33	PC25 (J.M.)	Not1-pSr33(without stop)-Apa1	Sr33 Prom NotI-F/ Sr33 PromR-ApaI	Plasmid (genomic DNA) from S.P. (10)	pVecNeo	Some fragments were ligated in pGEM-T easy vector	–
			Apa1-YFPv(with stop)-EcoR1	Venus ApaI Link-F/ Venus-full-length-R EcoRI	pAM-PAT-35s::GTW:YFPv		(Promega) and sequentially ligated in pVecNeo (Apa1/ BamH1 and Not1/Apa1)	
			EcoR1-Sr33ter-BamH1	Sr33 Term EcoRI-F/ Sr33 Term BamHI-R	Plasmid (genomic DNA) from S.P. (10)			
	pSr50::Sr50g:terSr50	Sr50g	–	–	–	–	–	(11)
	pSr50::Sr50:YFPv:terSr50	PC137 (C.C.)	PCR 1: Sr50 fragment including internal BaeI site and Sr50 c-ter (without stop)-XmaI-ApaI	Sr50F1/Sr50R1	Plasmid (genomic DNA) from R.M. (11)	pVecNeo	pGEM-T easy with Sr50 genomic sequence (11) was digested with BaeI and	–
			PCR 2: XmaI-PmeI-Sr50ter-ApaI	Sr50F2/Sr50R2	Plasmid (genomic DNA) from R.M. (11)		ApaI and ligated to PCR 1. PCR 2 was added using	
			PCR 3: XmaI-YFPv(with stop)-PmeI	VenusF/VenusR	pAM-PAT-35s::GTW:YFPv		XmaI/ApaI sites then PCR3 was added using XmaI/PmeI sites. The NotIpSr50::Sr50g: YFPv:terSr50-ApaI fragment was ligated into pVecNeo	
	pSr33::Sr33g:terSr33	Sr33g	–	–	–	–	–	(10)

*Max-Planck Institute, Cologne.